ERJ Express. Published on May 10, 2018 as doi: 10.1183/13993003.00236-2018

EUROPEAN RESPIRATORY *journal*

FLAGSHIP SCIENTIFIC JOURNAL OF ERS

Early View

Original article

Fibroblast Growth Factor 23 and Klotho Contribute to Airway Inflammation

Stefanie Krick, Alexander Grabner, Nathalie Baumlin, Christopher Yanucil, Scott Helton, Astrid Grosche, Juliette Sailland, Patrick Geraghty, Liliana Viera, Derek W. Russell, J. Michael Wells, Xin Xu, Amit Gaggar, Jarrod Barnes, Gwendalyn D. King, Michael Campos, Christian Faul, Matthias Salathe

Please cite this article as: Krick S, Grabner A, Baumlin N, *et al*. Fibroblast Growth Factor 23 and Klotho Contribute to Airway Inflammation. *Eur Respir J* 2018; in press (https://doi.org/10.1183/13993003.00236-2018).

Fibroblast Growth Factor 23 and Klotho Contribute to Airway Inflammation

Stefanie Krick[1], Alexander Grabner[2], Nathalie Baumlin[3], Christopher Yanucil[4], Scott Helton[1], Astrid Grosche[3], Juliette Sailland[3], Patrick Geraghty[5], Liliana Viera[1], Derek W. Russell[1], J. Michael Wells[1,6], Xin Xu[1], Amit Gaggar[1], Jarrod Barnes[1], Gwendalyn D. King[7], Michael Campos[3], Christian Faul[4*] and Matthias Salathe[3*].

[1]Division of Pulmonary, Allergy and Critical Care Medicine, Department of Medicine, The University of Alabama at Birmingham, Birmingham, AL, USA.

[2]Division of Nephrology, Department of Medicine, Duke University Medical Center, Duke University, Durham, USA.

[3]Division of Pulmonary, Critical Care and Sleep Medicine, Department of Medicine, University of Miami Leonard M. Miller School of Medicine, Miami, FL 33136, USA.

[4]Division of Nephrology, Department of Medicine, The University of Alabama at Birmingham, Birmingham, AL, USA.

[5]Division of Pulmonary and Critical Care Medicine, Department of Medicine, State University of New York Downstate Medical Center, Brooklyn, NY, USA

[6]UAB Lung Health Center

[7]Department of Neurobiology, The University of Alabama at Birmingham, Birmingham, AL, USA.

[*] Both senior authors contributed equally to this manuscript.

Correspondence should be addressed to:

Stefanie Krick, MD PhD,

Division of Pulmonary, Allergy and Critical Care Medicine,

Department of Medicine,

The University of Alabama at Birmingham,

1900 University Blvd., THT-422, Birmingham, AL 35294.

Tel.: 205-975-5341;

Fax: 205-934-1721;

E-mail: skrick@uabmc.edu

Take Home Message:

FGF23 and smoke induced FGF receptor 4 signaling lead to the development of airway inflammation and emphysema.

This article has an online data supplement.

ABSTRACT

Circulating levels of fibroblast growth factor (FGF) 23 are associated with systemic inflammation and increased mortality in chronic kidney disease. α-klotho, a co-receptor for FGF23, is downregulated in chronic obstructive pulmonary disease (COPD). However, whether FGF23 and klotho-mediated FGFR activation delineates a pathophysiologic mechanism in COPD remains unclear. We hypothesized that FGF23 can potentiate airway inflammation via klotho independent FGFR4 activation. FGF23 and its effect were studied using plasma and transbronchial biopsies from COPD and control patients and primary human bronchial epithelial cells isolated from COPD patients as well as a murine COPD model.

Plasma FGF23 levels were significantly elevated in COPD patients. Exposure of airway epithelial cells to cigarette smoke and FGF23 led to a significant increase in IL-1β release via klotho-independent FGFR4-mediated activation of phospholipase Cγ (PLCγ)/nuclear factor of activated T-cells (NFAT) signaling. In addition, klotho knockout mice developed COPD and showed airway inflammation and elevated FGFR4 expression in their lungs, whereas overexpression of klotho led to an attenuation of airway inflammation.

In conclusion, cigarette smoke induces airway inflammation by downregulation of klotho and activation of FGFR4 in the airway epithelium in COPD. Inhibition of FGF23 or FGFR4 might serve as a novel anti-inflammatory strategy in COPD.

INTRODUCTION

Chronic obstructive pulmonary disease (COPD) represents the third leading cause of global mortality according to the World Health Organization (http://www.who.int/gho/en/). Exposure to cigarette smoke is responsible for the majority of COPD cases and is the world's leading cause of avoidable premature mortality (1). Various studies have shown inflammatory changes in the airway epithelium in COPD and due to cigarette smoke, including goblet hyperplasia and increased expression of pro-inflammatory cytokines (2-4).

Fibroblast Growth Factor (FGF) 23**,** a 27 kDa protein secreted by osteocytes, plays an essential role in maintaining serum phosphate homeostasis (5-7). In chronic kidney disease (CKD), plasma concentrations of FGF23 are elevated and strongly associated with the risk of CKD progression, cardiovascular events and mortality (8,9). To date, direct effects of FGF23 on the lung have not been reported. However, it has been shown that klotho expression is reduced in airways from COPD patients (10). Recombinant klotho, a single-transmembrane protein that exists in a membrane bound and soluble form and acts as a FGF23 co-receptor, protects the alveolar epithelium against oxidative damage (11-13). Furthermore, mice lacking klotho develop an aging phenotype with widened alveolar spaces, consistent with pulmonary emphysema (14).

FGF receptors (FGFR) are a sub-family of receptor tyrosine kinases and consist of four isoforms (FGFR1-4) (15). In its classic target organs, such as kidney and the parathyroid gland, FGF23 signals via FGFR1 and requires klotho. By binding to FGFR1/klotho, FGF23 activates the Ras/mitogen-activated protein kinase (MAPK)

signaling pathway (16). In the absence of klotho, FGF23 can activate FGFR4 and induce subsequent PLCγ/NFAT signaling. This mechanism mediates pathophysiologic actions of FGF23 that include the induction of hypertrophic growth in cardiac myocytes and the increased production of inflammatory cytokines in hepatocytes (17,18).

We hypothesized that cigarette smoke contribute to increased production and activation of FGF23 signaling in COPD. Here, we examine whether cigarette smoke reduces klotho and increases FGFR4 expression resulting in pro-inflammatory PLCγ/NFAT signaling in human primary bronchial epithelial cells. We postulate that FGF23 can potentiate inflammation in the lung via activation of FGFR4 and downregulation of klotho.

RESULTS

Plasma FGF23 levels are increased in individuals with COPD

We measured FGF23 in plasma samples from 28 individuals, including 18 with COPD and 10 age-matched non-COPD patients. COPD was defined as a forced expiratory volume in 1-second to forced vital capacity (FEV1/FVC) < 0.70. The post-bronchodilator FEV1 percent predicted (FEV1%) was used to measure the severity of airflow obstruction, with a FEV1 ≥ 50% and ≤ 1 COPD exacerbation within the last year, indicating mild-to-moderate COPD (9 individuals) and a FEV1 < 50% and ≥ 2 COPD exacerbations within the last year, indicating severe COPD (9 individuals). The clinical characteristics, including age, sex, smoking history and percent predicted FEV1 (FEV1%) are shown in supplemental Table 1. As expected, the post bronchodilator FEV1% was significantly lower in both COPD groups when compared to controls.

Individuals with mild-to-moderate COPD had higher FGF23 plasma levels when compared to patients without COPD (59±12 versus 42±10 pg/ml, P=0.004; Fig. 1a). However, FGF23 was not significantly increased in severe COPD compared to controls in this study population (51 ± 18 versus 42±10 pg/ml, P=0.26). We therefore focused on mild-to-moderate COPD for further experimentations. We detected no difference between active smokers and non-smokers (Suppl. Fig. 1a).

Endobronchial biopsies from the mild-to-moderate subgroup with significantly elevated FGF23 levels showed bronchial epithelial cell metaplasia (Fig. 1b, upper panel). Tracheal sections from control and these COPD donors showed distinct FGF23 staining of the epithelial layer (Fig. 1b, lower panel). As expected, the COPD group had significantly increased goblet cell numbers when compared to the control group (Fig. 1c).

We observed significant increases in plasma IL-6 levels (Fig. 1d, left panel), and bronchoalveolar lavage fluid (BALF) IL-8 levels (Fig. 1d, right panel) were elevated in COPD patients. Determination of the Pearson correlation coefficient showed a significant positive correlation between plasma FGF23 levels and plasma IL-6 levels (R^2= 0.2224 with p=0.0415, Fig. 1d, lower left panel)) but no significant correlation between plasma FGF23 levels and BALF IL-8 levels (R^2= 0.01542 with p=0.7006, Fig. 1d, lower right panel). Combined, these data suggest that COPD patients develop increased plasma levels of FGF23, which coincide with elevated levels of inflammatory cytokines in the lung and circulation.

FGF23 and cigarette smoke induce IL-1β secretion in bronchial epithelial cells from individuals with COPD

To determine direct effects of FGF23 in combination with cigarette smoke, we exposed primary bronchial epithelial cells isolated from four different individuals with COPD (COPD-BEC) to cigarette smoke and FGF23 and assessed expression of IL-6, IL-8 and IL-1β by quantitative real time PCR. Overall, we observed a considerable heterogeneity in cytokine expression. IL-6 mRNA increased to FGF23 ± cigarette smoke with high variability (Fig. 2a); IL-8 was significantly increased with FGF23 ± cigarette smoke, but the increase was less variable and more modest (Fig. 2b). IL-1β mRNA levels were not significantly increased by FGF23 alone, but the combination of both stimuli led to an over 5-fold elevation (Fig. 2c). Exposure of COPD-BEC to either stimulus, however, caused a significant increase in basolateral secretion of IL-1β, which was further elevated, when both stimuli were combined (Fig. 2d). These findings indicate that, in combination with smoke, FGF23 can directly target COPD-BEC and induce the expression and release of IL-1β.

FGF23 activates FGFR4 and PLCγ/calcineurin/NFAT signaling in COPD-BEC resulting in increased IL-1β secretion

As shown in other tissues, FGF23 can induce both phosphorylation of PLCγ (19) and ERK (20) depending on the absence or presence of klotho. To determine whether FGF23 can activate FGFR4 and subsequent PLCγ/calcineurin/NFAT signaling and induce an inflammatory response in the lung, as we have recently shown in the liver (18), we analyzed FGFR4 binding to PLCγ after treatment with FGF23.

In COPD-BEC, stimulation with FGF23 + cigarette smoke caused phosphorylation of PLCγ, consistent with the premise that these effects might be mediated by klotho-independent FGFR4 signaling. On the other hand, FGF23 alone did not result in phosphorylation of ERK, an effect clearly associated with smoke exposure (Fig. 3a, left panel).

In order to verify this finding, endogenous PLCγ was immunoprecipitated and eluates analyzed by immunoblotting with an anti-FGFR4 antibody. Compared with eluates from control cells, levels of co-purified FGFR4 were elevated in FGF23-treated COPD-BEC while total PLCγ expression levels were unchanged. Pre-treatment with a FGFR4-specific blocking antibody (anti-FGFR4) (17) inhibited the co-immunoprecipitation of FGFR4 and PLCγ (Fig. 3a, right panel). Combined exposure of COPD-BEC to FGF23 and cigarette smoke also led to the phosphorylation of PLCγ which was blocked by anti-FGFR4 (Fig. 3b, left panel). Cigarette smoke, but not FGF23 stimulation by itself, caused a marked increase in ERK phosphorylation which has been shown before in bronchial epithelial cells (21). However, ERK phosphorylation was unchanged by pre-incubation with anti-FGFR4 (Fig. 3b left panel). These findings indicate that FGF23 signaling in the bronchial epithelium occurs mainly via activation of PLCγ rather than ERK and that this effect is mediated by FGFR4.

To determine if the FGFR4/PLCγ/calcineurin/NFAT signaling cascade mediates FGF23 effects on IL-1β expression, we pre-incubated COPD-BEC with anti-FGFR4 followed by stimulation with FGF23 and cigarette smoke. Anti-FGFR4 significantly reduced elevations in mRNA as well as secreted levels of IL-1β (Fig. 3b, middle panel). To establish the link between FGF23 and NFAT activation, we employed the widely used

calcineurin inhibitor, cyclosporine A (CsA) (17,18) and showed that CsA also inhibited the FGF23 and CS induced IL-1β responses (Fig. 3b, right panel). Furthermore, mRNA levels of cyclooxygenase (COX) 2, a described NFAT target gene in the bronchial epithelium (22), were increased following co-stimulation with FGF23 and smoke. This effect was inhibited when cells were pre-treated with CsA (Fig. 3c). Additionally, we used the bronchial epithelial cell line 16HBE and transfected these cells with a NFAT reporter gene luciferase construct. An increase in NFAT activity was seen after stimulation with FGF23, which was significantly inhibited when cells were pre-incubated with anti-FGFR4 and CsA. Furthermore, cigarette smoke extract (CSE) and CSE+FGF23 also induced NFAT activation, which could be blocked by CsA (Fig. 3c, middle panel).

We identified NFAT2c and 3c as the most abundant isoforms in COPD-BEC, HBEC and 16HBE cells (Fig. 3c, middle and right panel). To further validate the specificity of FGF23 induced NFAT activation, both isoforms were knocked down by using siRNA in 16HBE cells (Fig. 3d). Since these 16HBE cells showed a similar IL-1β response as the primary cells, we stimulated control, siNFAT2c and 3c transfected 16 HBE cells with CSE and FGF23. SiNFAT2c decreased both NFAT2c and 3c, while siNFAT3c was isoform-specific. Compared to si control transfected cells, the CSE+FGF23 induced IL-1β response was blunted in siNFAT2c and siNFAT3c transfected cells (Fig. 3d, middle panel). This indicates that both NFAT2c and NFAT3c are mediators of FGF23-induced signaling. Furthermore, CSE ± FGF23 led to a significant increase in FGFR4 protein expression levels in 16HBE cells (Fig. 3d, right panel). Combined, our results show that FGF23 directly activates FGFR4/PLCγ/calcineurin/NFAT signaling in bronchial epithelial cells thereby inducing IL-1β.

Exposure to cigarette smoke downregulates klotho expression and upregulates FGFR4 in bronchial epithelial cells from individuals with COPD

Since klotho expression is decreased in COPD airways (10), we analyzed klotho expression in our primary air liquid interface bronchial epithelial cell culture system. Exposure of COPD-BEC to cigarette smoke caused a significant decrease in klotho protein and mRNA levels, whereas FGF23 alone had no effect (Fig. 4a). Compared to HBEC derived from non-smoker and non-COPD lungs, klotho mRNA and protein levels were significantly reduced in COPD-BEC (Fig. 4b). These data show that in COPD-BEC, klotho expression is decreased and further reduced by cigarette smoke, indicating that both COPD and smoke might serve as factors that promote klotho-independent FGF23 signaling in the lung.

We measured FGFR4 expression in the lung, as FGFR4 has been previously shown to mediate the klotho-independent FGF23 signaling in the heart and liver (17,18). Paraffin embedded endobronchial biopsies were used for hematoxylin staining and FGFR4 immunohistochemistry. FGFR4 staining was localized to the bronchial epithelium and appeared to be increased in endobronchial tissue biopsies from COPD patients (Fig. 4c, left panel). To better quantify FGFR4 expression, FGFR4 mRNA levels were determined and showed a significant increase in COPD-BEC compared to control HBEC (Fig. 4c, right panel).

Next, COPD-BEC were exposed to an increasing number of cigarette puffs. A dose dependent upregulation of FGFR4 protein and mRNA levels was detected after 24 hours (Fig. 4d). Taken together, FGFR4 is expressed in the bronchial epithelium and upregulated in COPD patients and upon exposure to cigarette smoke.

Klotho deficiency leads to increased FGFR4 activation and inflammation

As genetic mouse models lacking klotho develop elevated serum FGF23 levels, we wanted to determine if klotho-independent FGF23 signaling and associated inflammation occur in the lungs of these animals. As shown by others before (12), we observed widened airway spaces on H&E staining (Fig. 5a) by immunohistochemical characterization of the klotho hypomorphic mice ($kl^{-/-}$) (Fig. 5a).

Mean linear intercept (MLI x 1000 in μm) analysis was used to quantify airspace enlargement, which was significantly higher in klotho deficient mouse lungs compared to wild type ($kl^{+/+}$) littermates (Fig. 5a, upper panel). Furthermore, FGF23 mRNA levels were upregulated in in $kl^{-/-}$ lungs when compared to $kl^{+/+}$ (Fig. 5a, lower panel). Immunhistochemical analysis of lung sections using anti-FGF23 showed an intense signal in the bronchial epithelium (Fig. 5b, right panel). When compared to their wild type litter mates, bronchoalveolar lavage fluid (BALF) from $kl^{-/-}$ mice contained more cells, specifically neutrophils (23) and macrophages/monocytes (Fig. 5c). There was no difference in the number of lymphocytes between both groups (Fig. 5c), but IL-6 mRNA levels were also increased (Fig. 5c). To determine the activity of FGFR4/PLCγ, we immunoprecipitated PLCγ from mouse lung tissue extracts followed by immunoblotting of eluates for FGFR4. We found an increase in co-purified FGFR4 in lungs from $kl^{-/-}$ mice when compared to wild type littermates (Fig. 5d, left panel). Furthermore, FGFR4 mRNA levels were increased in cultured, fully differentiated murine tracheal epithelial cells (MTEC) from $kl^{-/-}$ mice (Fig. 5d, middle panel). They also showed a significantly increased basolateral secretion of IL-6 (Fig. 5d, right panel). These findings indicate that

in the absence of klotho and in the presence of elevated FGF23, FGFR4/PLCγ signaling and production of inflammatory cytokines are elevated in the mouse lung.

Soluble klotho protects COPD-BECs from pro-inflammatory effects of FGF23 and smoke

The extracellular domain of klotho can exist in a soluble form (24). It has been shown that soluble klotho has protective, anti-inflammatory effects on different cell types (25,26). To test if soluble klotho interferes with the effects of FGF23 in the lung, we co-incubated COPD-BEC with FGF23, cigarette smoke and with the ectodomain of recombinant human α-klotho at 0.1 μg/ml for 30 minutes. As shown before, FGF23+CS caused an increase in PLCγ phosphorylation without affecting total PLCγ levels. In the presence of FGF23 and cigarette smoke, treatment of COPD-BEC with soluble klotho also led to a decrease in IL-1β secretion (Fig. 6b).

Overexpression or knockdown of klotho in mice alters FGF23/FGFR4 signaling.

Since mice that were exposed to chronic cigarette smoke (27) did not show an upregulation of FGF23 serum levels (Suppl. Fig. 1b), we used an acute mouse model for cigarette smoke exposure. Mice were exposed to one week of cigarette smoke to induce acute airway inflammation. Western blot analyses of total lung tissue showed in some mice an increase in FGF23 levels (Fig. 7a: 6/11 mice in smoke exposure, 3/11 mice in controls) (Fig. 7a). However, there was no significant increase in serum FGF23 levels between the control and smoked-exposed groups (Fig 7a), and there was no significant

difference in mRNA levels of klotho or FGFR4 in lung tissue (Fig. 7a). When comparing wild type mice and klotho overexpressing mice (WT, OE) (28), the later group showed increased klotho mRNA levels in the lung, which was independent of smoke exposure (Fig. 7b). We detected no difference in serum FGF23 levels and in BALF total cell count (Fig. 7b). Smoke-induced increase of IL-6 in the lung was decreased in the klotho overexpressing mice when compared to wild type littermates (Fig. 7b). To test the effect of klotho deficiency and since $kl^{-/-}$ mice were too sick to be exposed to cigarette smoke, MTECs were isolated from both $kl^{+/+}$ and $kl^{-/-}$ mice. At baseline, $kl^{-/-}$ MTECs had higher mRNA levels of IL-6 and fgfr4 when compared to wild type cells (Fig. 7c).

To further characterize the link between klotho deficiency, FGF23 increase and elevated FGFR4 expression as direct or indirect, MTECs from fgfr4 constitutively active transgenic (TG) mice were analyzed and did not show any difference in IL-6 levels compared to control MTECs. Interestingly, there was also a trend toward an increase in klotho mRNA levels in these fgfr4 TG MTECs (Suppl Fig. 2a and b). MTEcs from $fgfr4^{-/-}$ mice though showed protection from FGF23 and CS induced IL-6 increase accompanied by a downregulation of klotho expression (Suppl. Fig. 2c and d).

In summary, our findings indicate that in COPD, there is smoke induced upregulation of FGFR4 expression and a decrease in soluble klotho, enabling elevated FGF23 to signal via FGFR4/PLCγ/NFAT to induce airway inflammation (Fig. 8). Furthermore, co-administration with soluble klotho can block FGF23-mediated signaling in COPD-BEC thereby inhibiting the pro-inflammatory actions of FGF23.

DISCUSSION

Here, we show for the first time FGF23-induced signaling in the bronchial epithelium and provide new insights into the opposing roles of FGF23 and its co-receptor klotho in cigarette smoke-induced chronic bronchitis. We demonstrate that 1) plasma FGF23 levels are elevated in patients with mild-to-moderate COPD and an associated inflammatory phenotype with goblet cell hyperplasia, 2) cigarette smoke exposure in combination with FGF23 induces IL-1β secretion from primary human bronchial epithelial cell cultures from COPD patients, 3) cigarette smoke induces an increase of FGFR4 and a decrease of klotho expression thereby causing activation of PLCγ/NFAT signaling and inflammation, and 4) the presence of soluble klotho attenuates smoke-induced IL-1β secretion.

A positive correlation between plasma FGF23 levels and smoking has been described previously using a multivariable regression analysis of 604 patients with CKD (29). However, in this study the smokers were not further characterized regarding COPD. In a different report, increased FGF23 levels in COPD patients were linked to hypophosphatemia, but a mechanism for elevation and the source of circulating FGF23 was not identified (30). Here, we show that FGF23 levels appear not to correlate with disease severity per se, since there is no systemic FGF23 elevation in patients with severe COPD. One explanation could be that FGF23/klotho perturbations may decrease in advanced disease due to “burn-out” as the residual mass of viable lung epithelium decreases. If this is the case, FGF23/klotho dysregulation may effectively represent a marker not only of disease but also for “at risk” lung tissue mass. Therefore, we focused on the group of these patients with mild-to-moderate COPD by assessing inflammation in their plasma and transbronchial biopsy specimens. Klotho, a co-receptor for FGF23, is

downregulated in airway epithelial cells from COPD patients (10). In addition, previous reports showed that gene silencing of klotho in a bronchial epithelial cell line induces IL-8 secretion which is further enhanced by cigarette smoke extract (10).

Our data also show that in a COPD mouse model (due to deficiency of klotho), there is increased bronchial inflammation, which is at least partially generated by the bronchial epithelial cells and an influx of macrophages and neutrophils. We further characterize the underlying novel signaling pathway for smoke-induced inflammatory airway disease that has the potential for future therapeutic intervention, namely FGFR4 activation and consecutive PLCγ/calcineurin/NFAT signaling which occurs in a state of klotho deficiency and upregulation of FGF23. It is challenging to experimentally characterize the link between klotho deficiency, and our data indicate that regulation of both is tightly linked. It has been shown previously that klotho knockout mice have elevated FGF23 levels (19). Currently, it is not clear how soluble klotho blocks the FGF23 effects in bronchial epithelial cells, since ERK phosphorylation is not altered. However, we showed that soluble klotho is not a circulating co-receptor for FGF23 in the lung that mediates ERK signaling. Therefore, further studies are needed.

Interestingly, we also observed ERK activation in cigarette smoke-induced IL-1β expression, which appears to be FGF23/FGFR4 independent, as there was no change after pre-incubation with a FGFR4 inhibitor (Fig. 3b). Since cigarette smoke downregulates klotho expression, FGF23 signaling occurs via FGFR4 as we have previously demonstrated in the liver and in the myocardium (17,18). This ultimately leads to an increase in IL-1β secretion, a key cytokine in virus-induced lung disease (31). Administration of an IL-1β antibody reduces lung inflammation in a mouse model of

influenza (32). Furthermore, IL-1β is elevated in total lung tissue and sputum from COPD patients (33) and associated with frequent COPD exacerbations as well as an IL-1β-associated sputum proteomic signature (34,35).

The importance of identifying new COPD-related signaling pathways is required for future therapeutic strategies. FGFRs are ubiquitously expressed, whereas FGFR4 is mainly found in lung, heart, kidney and liver. Signaling via FGFR4 is associated with inflammatory changes and we demonstrate several links of FGFR4 signaling to airspace remodeling and inflammation. In addition, a FGFR4 blocking antibody and small molecule inhibitors have been developed for the treatment of hepatocellular carcinomas (36,37). Therefore, therapeutically targeting FGFR4 or soluble klotho levels in the inflammatory subtypes of COPD may represent novel therapeutic options.

METHODS

Please refer to Supplementary Material for further methodological details.

Study Approval

The clinical study was conducted according to the principles of the Declaration of Helsinki and was approved by the University of Miami Institutional Review Board. Written informed consent was received from each participant prior to inclusion in the study. Human airways were obtained from organ donors whose lungs were rejected for transplant. Institutional Review Board-approved consent for research was obtained by the Life Alliance Organ Recovery Agency of the University of Miami or the LifeCenter Northwest and conformed to the Declaration of Helsinki. All animal protocols were

approved by the Institutional Animal Care and Use Committees at the University of Miami and the University of Alabama at Birmingham.

IL-1β, IL-6 and IL-8 ELISA and mRNA assessment

An ultrasensitive IL-1β and IL-6 enzyme-linked immunosorbent assay (ELISA) from Invitrogen (Thermo Fisher Scientific) was used. HBEC were stimulated with FGF23 ± cigarette smoke (25 ng/ml and 4 cigarettes for 24 h) and 100 µl of the basolateral medium (undiluted) was used for measurements. Gene expression was performed by qPCR using Taqman probes (Life technologies/Applied Biosystems, Carlsbad, CA, USA).

Statistics

Data were analyzed with Prism5 (GraphPad Software, Inc., La Jolla, CA) and shown as mean ± SEM using Student's *t* test and analysis of variance or Kruskal Wallis H test with one-way ANOVA with appropriate post tests for at least three independent experiments. Significance was accepted at $p < 0.05$.

ACKNOWLEDGEMENTS

The authors thank J.S. Dennis, D. Duncan and S. Hutcheson for technical assistance. They also thank G. Holt and E. Donna for assisting in obtaining the bronchoscopic specimen used in this study and R. Abraham and J. Bange (U3 Pharma) for providing the anti-FGFR4 blocking antibody. This work was supported by the Flight Attendant Medical Research Institute (YFAC152003 to S.K., YCSA113380 to P.G. and CIA13033 to M.S.), the Cystic Fibrosis Foundation (CFF KRICK1610 to S.K. and SALATH14G0 to M.S.), the American Heart Association (A.G., C.F.), the American Diabetes Association (C.F.),

the James & Esther King Florida Biomedical Research Program (5JK02 to M.S.) and the NIH (R01HL128714 to C.F.).

REFERENCES

1. Samet, J. M. (2013) Tobacco smoking: the leading cause of preventable disease worldwide. *Thorac Surg Clin* **23**, 103-112
2. de Boer, W. I., Sont, J. K., van Schadewijk, A., Stolk, J., van Krieken, J. H., and Hiemstra, P. S. (2000) Monocyte chemoattractant protein 1, interleukin 8, and chronic airways inflammation in COPD. *J Pathol* **190**, 619-626
3. Polosukhin, V. V. (2001) Ultrastructural of the bronchial epithelium in chronic inflammation. *Ultrastruct Pathol* **25**, 119-128
4. Mortaz, E., Henricks, P. A., Kraneveld, A. D., Givi, M. E., Garssen, J., and Folkerts, G. (2011) Cigarette smoke induces the release of CXCL-8 from human bronchial epithelial cells via TLRs and induction of the inflammasome. *Biochimica et biophysica acta* **1812**, 1104-1110
5. Schiavi, S. C., and Kumar, R. (2004) The phosphatonin pathway: new insights in phosphate homeostasis. *Kidney Int* **65**, 1-14
6. Mirams, M., Robinson, B. G., Mason, R. S., and Nelson, A. E. (2004) Bone as a source of FGF23: regulation by phosphate? *Bone* **35**, 1192-1199
7. Benet-Pages, A., Lorenz-Depiereux, B., Zischka, H., White, K. E., Econs, M. J., and Strom, T. M. (2004) FGF23 is processed by proprotein convertases but not by PHEX. *Bone* **35**, 455-462
8. Gutierrez, O. M., Mannstadt, M., Isakova, T., Rauh-Hain, J. A., Tamez, H., Shah, A., Smith, K., Lee, H., Thadhani, R., Juppner, H., and Wolf, M. (2008) Fibroblast growth factor 23 and mortality among patients undergoing hemodialysis. *N Engl J Med* **359**, 584-592

9. Shimada, T., Urakawa, I., Isakova, T., Yamazaki, Y., Epstein, M., Wesseling-Perry, K., Wolf, M., Salusky, I. B., and Juppner, H. (2010) Circulating fibroblast growth factor 23 in patients with end-stage renal disease treated by peritoneal dialysis is intact and biologically active. *J Clin Endocrinol Metab* **95**, 578-585

10. Gao, W., Yuan, C., Zhang, J., Li, L., Yu, L., Wiegman, C. H., Barnes, P. J., Adcock, I. M., Huang, M., and Yao, X. (2015) Klotho expression is reduced in COPD airway epithelial cells: effects on inflammation and oxidant injury. *Clinical science* **129**, 1011-1023

11. Ravikumar, P., Ye, J., Zhang, J., Pinch, S. N., Hu, M. C., Kuro-o, M., Hsia, C. C., and Moe, O. W. (2014) alpha-Klotho protects against oxidative damage in pulmonary epithelia. *Am J Physiol Lung Cell Mol Physiol* **307**, L566-575

12. Kuro-o, M., Matsumura, Y., Aizawa, H., Kawaguchi, H., Suga, T., Utsugi, T., Ohyama, Y., Kurabayashi, M., Kaname, T., Kume, E., Iwasaki, H., Iida, A., Shiraki-Iida, T., Nishikawa, S., Nagai, R., and Nabeshima, Y. I. (1997) Mutation of the mouse klotho gene leads to a syndrome resembling ageing. *Nature* **390**, 45-51

13. Chen, G., Liu, Y., Goetz, R., Fu, L., Jayaraman, S., Hu, M. C., Moe, O. W., Liang, G., Li, X., and Mohammadi, M. (2018) alpha-Klotho is a non-enzymatic molecular scaffold for FGF23 hormone signalling. *Nature* **553**, 461-466

14. Suga, T., Kurabayashi, M., Sando, Y., Ohyama, Y., Maeno, T., Maeno, Y., Aizawa, H., Matsumura, Y., Kuwaki, T., Kuro, O. M., Nabeshima, Y., and Nagai, R. (2000) Disruption of the klotho gene causes pulmonary emphysema in mice.

Defect in maintenance of pulmonary integrity during postnatal life. *Am J Respir Cell Mol Biol* **22**, 26-33

15. Faul, C. (2016) Cardiac actions of fibroblast growth factor 23. *Bone*
16. Urakawa, I., Yamazaki, Y., Shimada, T., Iijima, K., Hasegawa, H., Okawa, K., Fujita, T., Fukumoto, S., and Yamashita, T. (2006) Klotho converts canonical FGF receptor into a specific receptor for FGF23. *Nature* **444**, 770-774
17. Grabner, A., Amaral, A. P., Schramm, K., Singh, S., Sloan, A., Yanucil, C., Li, J., Shehadeh, L. A., Hare, J. M., David, V., Martin, A., Fornoni, A., Di Marco, G. S., Kentrup, D., Reuter, S., Mayer, A. B., Pavenstadt, H., Stypmann, J., Kuhn, C., Hille, S., Frey, N., Leifheit-Nestler, M., Richter, B., Haffner, D., Abraham, R., Bange, J., Sperl, B., Ullrich, A., Brand, M., Wolf, M., and Faul, C. (2015) Activation of Cardiac Fibroblast Growth Factor Receptor 4 Causes Left Ventricular Hypertrophy. *Cell metabolism* **22**, 1020-1032
18. Singh, S., Grabner, A., Yanucil, C., Schramm, K., Czaya, B., Krick, S., Czaja, M. J., Bartz, R., Abraham, R., Di Marco, G. S., Brand, M., Wolf, M., and Faul, C. (2016) Fibroblast growth factor 23 directly targets hepatocytes to promote inflammation in chronic kidney disease. *Kidney international*
19. Faul, C., Amaral, A. P., Oskouei, B., Hu, M. C., Sloan, A., Isakova, T., Gutierrez, O. M., Aguillon-Prada, R., Lincoln, J., Hare, J. M., Mundel, P., Morales, A., Scialla, J., Fischer, M., Soliman, E. Z., Chen, J., Go, A. S., Rosas, S. E., Nessel, L., Townsend, R. R., Feldman, H. I., St John Sutton, M., Ojo, A., Gadegbeku, C., Di Marco, G. S., Reuter, S., Kentrup, D., Tiemann, K., Brand, M., Hill, J. A., Moe, O. W., Kuro, O. M., Kusek, J. W., Keane, M. G., and Wolf, M. (2011)

FGF23 induces left ventricular hypertrophy. *The Journal of clinical investigation* **121**, 4393-4408

20. Olauson, H., Lindberg, K., Amin, R., Sato, T., Jia, T., Goetz, R., Mohammadi, M., Andersson, G., Lanske, B., and Larsson, T. E. (2013) Parathyroid-specific deletion of Klotho unravels a novel calcineurin-dependent FGF23 signaling pathway that regulates PTH secretion. *PLoS genetics* **9**, e1003975
21. Xu, X., Balsiger, R., Tyrrell, J., Boyaka, P. N., Tarran, R., and Cormet-Boyaka, E. (2015) Cigarette smoke exposure reveals a novel role for the MEK/ERK1/2 MAPK pathway in regulation of CFTR. *Biochimica et biophysica acta* **1850**, 1224-1232
22. Ding, J., Li, J., Xue, C., Wu, K., Ouyang, W., Zhang, D., Yan, Y., and Huang, C. (2006) Cyclooxygenase-2 induction by arsenite is through a nuclear factor of activated T-cell-dependent pathway and plays an antiapoptotic role in Beas-2B cells. *The Journal of biological chemistry* **281**, 24405-24413
23. Krick, S., Baumlin, N., Aller, S. P., Aguiar, C., Grabner, A., Sailland, J., Mendes, E., Schmid, A., Qi, L., David, N. V., Geraghty, P., King, G., Birket, S. E., Rowe, S. M., Faul, C., and Salathe, M. (2017) Klotho Inhibits Interleukin-8 Secretion from Cystic Fibrosis Airway Epithelia. *Sci Rep* **7**, 14388
24. Hu, M. C., Shi, M., Zhang, J., Quinones, H., Griffith, C., Kuro-o, M., and Moe, O. W. (2011) Klotho deficiency causes vascular calcification in chronic kidney disease. *J Am Soc Nephrol* **22**, 124-136
25. Blake, D. J., Reese, C. M., Garcia, M., Dahlmann, E. A., and Dean, A. (2015) Soluble extracellular Klotho decreases sensitivity to cigarette smoke induced cell

death in human lung epithelial cells. *Toxicology in vitro : an international journal published in association with BIBRA* **29**, 1647-1652

26. Li, L., Wang, Y., Gao, W., Yuan, C., Zhang, S., Zhou, H., Huang, M., and Yao, X. (2015) Klotho Reduction in Alveolar Macrophages Contributes to Cigarette Smoke Extract-induced Inflammation in Chronic Obstructive Pulmonary Disease. *The Journal of biological chemistry* **290**, 27890-27900
27. Foronjy, R. F., Salathe, M. A., Dabo, A. J., Baumlin, N., Cummins, N., Eden, E., and Geraghty, P. (2016) TLR9 expression is required for the development of cigarette smoke-induced emphysema in mice. *American journal of physiology. Lung cellular and molecular physiology* **311**, L154-166
28. Li, Q., Vo, H. T., Wang, J., Fox-Quick, S., Dobrunz, L. E., and King, G. D. (2017) Klotho regulates CA1 hippocampal synaptic plasticity. *Neuroscience* **347**, 123-133
29. Vervloet, M. G., van Zuilen, A. D., Heijboer, A. C., ter Wee, P. M., Bots, M. L., Blankestijn, P. J., Wetzels, J. F., and study, M. g. (2012) Fibroblast growth factor 23 is associated with proteinuria and smoking in chronic kidney disease: an analysis of the MASTERPLAN cohort. *BMC nephrology* **13**, 20
30. Elsammak MY, A. A., Suleman M. . (2012) Fibroblast growth factor-23 and hypophosphatemia in chronic obstructive pulmonary disease patients. *J Med Biochem.* **31**, 12-18
31. Kim, K. S., Jung, H., Shin, I. K., Choi, B. R., and Kim, D. H. (2015) Induction of interleukin-1 beta (IL-1beta) is a critical component of lung inflammation during influenza A (H1N1) virus infection. *Journal of medical virology* **87**, 1104-1112

32. Indalao, I. L., Sawabuchi, T., Takahashi, E., and Kido, H. (2016) IL-1beta is a key cytokine that induces trypsin upregulation in the influenza virus-cytokine-trypsin cycle. *Archives of virology*

33. Pauwels, N. S., Bracke, K. R., Dupont, L. L., Van Pottelberge, G. R., Provoost, S., Vanden Berghe, T., Vandenabeele, P., Lambrecht, B. N., Joos, G. F., and Brusselle, G. G. (2011) Role of IL-1alpha and the Nlrp3/caspase-1/IL-1beta axis in cigarette smoke-induced pulmonary inflammation and COPD. *The European respiratory journal* **38**, 1019-1028

34. Fu, J. J., McDonald, V. M., Baines, K. J., and Gibson, P. G. (2015) Airway IL-1beta and Systemic Inflammation as Predictors of Future Exacerbation Risk in Asthma and COPD. *Chest* **148**, 618-629

35. Damera, G., Pham, T. H., Zhang, J., Ward, C. K., Newbold, P., Ranade, K., and Sethi, S. (2016) A Sputum Proteomic Signature That Associates with Increased IL-1beta Levels and Bacterial Exacerbations of COPD. *Lung* **194**, 363-369

36. Hagel, M., Miduturu, C., Sheets, M., Rubin, N., Weng, W., Stransky, N., Bifulco, N., Kim, J. L., Hodous, B., Brooijmans, N., Shutes, A., Winter, C., Lengauer, C., Kohl, N. E., and Guzi, T. (2015) First Selective Small Molecule Inhibitor of FGFR4 for the Treatment of Hepatocellular Carcinomas with an Activated FGFR4 Signaling Pathway. *Cancer discovery* **5**, 424-437

37. Ho, H. K., Pok, S., Streit, S., Ruhe, J. E., Hart, S., Lim, K. S., Loo, H. L., Aung, M. O., Lim, S. G., and Ullrich, A. (2009) Fibroblast growth factor receptor 4 regulates proliferation, anti-apoptosis and alpha-fetoprotein secretion during

hepatocellular carcinoma progression and represents a potential target for therapeutic intervention. *Journal of hepatology* **50**, 118-127

FIGURE LEGENDS

Figure 1. *FGF23 levels are increased in patients with mild-to-moderate COPD who have goblet cell hyperplasia and increased levels of pro-inflammatory cytokines.* (a) FGF23 plasma levels in non-COPD and COPD patients divided in mild-to-moderate and severe COPD and comparison of their FGF23 plasma levels. (b) Hematoxylin (upper row) and anti-FGF23 (lower row) staining of representative endobronchial biopsies from 1 control subject (left row) and 2 (middle and right row) subjects with mild-to-moderate COPD (20X magnification) with scale bar = 40 μm. (c) Quantification of goblet cells per field of view shows a significant increase in mild-to-moderate COPD when compared to subjects without COPD (n=6 of each group). (d) IL-6 plasma levels (left panel) and IL-8 levels in BALF (right panel) and dot blots showing their correlation with FGF23 levels in control subjects and patients with mild COPD (n = 6 of each group). Statistical analysis was done using Student's t test showing mean ± S.E.M. or ANOVA with *P<0.05 and **P<0.01 and for correlation analysis the Pearson correlation coefficient.

Figure 2. *Effect of cigarette smoke and FGF23 on expression of pro-inflammatory cytokines in COPD-BEC.* (a) mRNA levels of IL-6 and (b) IL-8 in COPD-BEC 24h after stimulation with cigarette smoke (4 cigarettes) ± FGF23 (25 ng/ml). (c) IL-1β mRNA and (d) secreted protein levels in the basolateral media from COPD-BEC after stimulation with FGF23, CS or both. Data are represented as fold change in mRNA or protein expression with n = 3 independent experiments from 6 different lungs. All bar graphs are mean ± S.E.M. *P<0.05, **P<0.01 and ***P<0.005, compared to control (ctrl) group.

Figure 3. *FGF23 induces activation of FGFR4/PLCγ/NFAT signaling in COPD-BEC.* (a) Left panel: Representative immunoblot and densitometric analysis (p-PLCγ/total PLCγ/actin ratio with n = 3) shows FGF23 + CS-induced phosphorylation of PLCγ (FGF23- and smoke dependent) and of ERK (purely smoke dependent). Right panel: Immunoblot of co-immunoprecipitation with FGFR4 using an anti-PLCγ antibody shows activation of PLCγ after FGF23 stimulation in COPD-BEC, which could be inhibited by pre-incubation with anti-FGFR4. (b) CS + FGF23 induce PLCγ and ERK phosphorylation as seen above but anti-FGFR4 only inhibits PLCγ phosphorylation. Both anti-FGFR4 and cyclosporine A (CsA), a calcineurin inhibitor, inhibit CS + FGF23-mediated induction of IL-1β mRNA and secreted protein levels. (c) CsA also attenuates induction of COX2 mRNA. FGF23, CSE alone and both activate NFAT, as assessed by a luciferase-based reporter gene assay in 16HBE cells, which can be blocked by CsA. Anti-FGFR4 inhibits FGF23-induced NFAT activation. The right two bar diagrams indicate mRNA levels of NFAT isoforms in both HBEC from nonsmokers and COPD patients as well as 16HBE cells. (d) siRNA targeting NFAT isoforms NFAT2c and NFAT3c were transfected into 16HBE cells. siNFAT2c reduces the expression of NFAT2c and NFAT3c, whereas siNFAT3c is specific for NFAT3c (left panel). When 16HBE cells were stimulated with FGF23 (20 ng/ml), CSE (5%) or both for 24 hours, IL-1β increased (second to right panel). Finally, the effects of siNFAT2c (knockdown of both the 2c and 3c isoforms) and siNFAT3c transfection were assessed after stimulation with CSE+FGF23 (middle panel). CSE±FGF23 also led to significant upregulation of FGFR4 protein expression in 16HBE cells. All n = 3 independent experiments (from 3 different

lungs in the case of COPD-BEC) showing mean ± S.E. with *P<0.05, **P<0.01 and ***P<0.005.

Figure 4. *Cigarette smoke exposure regulates expression of klotho and FGFR4 in COPD airway epithelia.* (a) Representative immunoblot showing downregulation of klotho protein and bar graphs indicating mRNA levels from COPD-BEC after treatment with CS, FGF23 or both stimuli for 24h. (b) Representative immunoblot and klotho mRNA levels of HBEC from nonsmokers compared to COPD-BEC. (n = 3 independent experiments from 6 different lungs. (c) Immunohistochemistry for FGFR4 and counterstaining with hematoxylin of endobronchial biopsies from 2 representative control patients and 2 COPD patients, compared to a negative control (upper left corner, 20X magnification). Bar graphs showing increased FGFR4 mRNA expression in COPD-BECs compared to control lungs. (d) Immunoblot analysis of FGFR4 protein levels (representative blot from 1 COPD patient, tested in 3 different COPD lungs) and quantitative real time PCR of FGFR4 mRNA levels in COPD-BECs 24h after exposure to 2, 4 and 6 cigarettes (1 cigarette = 6 puffs). (All n = 3 independent experiments from 3 different lungs showing mean ± S.E.M. with **P<0.01 and ***P<0.001).

Figure 5. *Loss of klotho expression causes increased airway inflammation in mice.* (a) Hematoxylin and anti-FGF23 staining of lung tissue from wild type ($kl^{+/+}$) and hypomorphic klotho ($kl^{-/-}$) mice (4X magnification). (b) Mean linear intercept analysis demonstrates widened airspaces in the $kl^{-/-}$ lung samples and FGF23 mRNA levels are upregulated in whole lung tissue from $kl^{-/-}$ when compared to $kl^{+/+}$ mice (6 mice for each group) (left panel). Immunohistochemical staining using anti-FGF23 in paraffin

embedded mouse lung tissue sections indicates a signal in the bronchial epithelium (right panel). (c) Assessment of total cells in BALF from $kl^{+/+}$ versus $kl^{-/-}$ mice (4 mice for each group). Also shown are BALF macrophage/monocyte count, BALF lymphocyte count x 10^4 per ml BAL fluid and IL-6 fold changes in BALF from $kl^{+/+}$ versus $kl^{-/-}$ mice. (d) Co-immunoprecipitation of endogenous FGFR4 by using anti-PLC-γ or anti-GFP (control) in lung tissue lysates from either $kl^{-/-}$ or $kl^{+/+}$ mice indicates increased fgfr4 in $kl^{-/-}$ lungs. qRT-PCR for FGFR4 mRNA in $kl^{-/-}$ MTEC showed a significant upregulation when compared to wild type MTEC and IL-6 protein levels in basolateral media from $kl^{+/+}$ and $kl^{-/-}$ MTEC. (Shown are means ± S.E.M. with *P<0.05, **P<0.01 and ***P<0.001; for mouse experiments, three different independent experiments were done; for each experiment, cells were pooled from 3-4 animals and morphometry and BALF analysis was done from 4 mice in each group).

Figure 6. *Supplementation of human recombinant klotho inhibits CS and FGF23-induced IL-1β secretion.* (a) Representative immunoblots show FGF23 (25 ng/ml for 30 min) induced phosphorylation of PLCγ. Inhibition of PLCγ phosphorylation occurs by pre-incubation with klotho (1 μg /ml, lane 3 and 0.1 μg /m, lane 4). (b) Soluble klotho inhibits CS+FGF23-mediated increases of IL-1β protein levels, assessed by ELISA from basolateral media. (All n = 3 independent experiments from 3 different lungs showing mean ± S.E. with **P<0.01).

Figure 7. *Effect of klotho overexpression and klotho deficiency on FGF23 signaling in mice.* (a) Representative immunoblots show FGF23 protein levels in total lung lysates from control mice and mice acutely exposed to cigarette smoke (CS). Bar graphs

demonstrating serum FGF23 levels, total lung klotho and FGFR4 mRNA levels in both mouse groups (b) Klotho mRNA levels, serum FGF23 levels, BAL fluid total cell count and CS-induced fold increase in total mouse lung IL-6 expression after exposure to acute CS and compared to non-exposed control mice (both wild type and klotho overexpressing mice). c) Bar graphs indicate IL-6 and FGFR4 transcript levels of MTECs isolated from $kl^{+/+}$ and $kl^{-/-}$ mice (Means are shown ± SEM with **p<0.01 and ***p<0.005).

Figure 8. *Possible signaling mechanism for cigarette smoke and FGF23-mediated regulation of FGFR4/PLCγ/calcineurin/NFAT pathway.* Diagram illustrating the direct effects of FGF23 and cigarette smoke on the COPD airway epithelium: cigarette smoke induces upregulation of FGFR4 and decreases klotho expression in the bronchial epithelium. In combination with elevated FGF23 plasma levels in COPD activates FGFR4/PLCγ/calcineurin/NFAT signaling to release IL-1β thereby inducing inflammation. Definition of Abbreviations: IL=interleukin, FGF=fibroblast growth factor, FGFR= FGF receptor, NFAT= Nuclear factor of activated T-cells, PLC=phospholipase C.

a

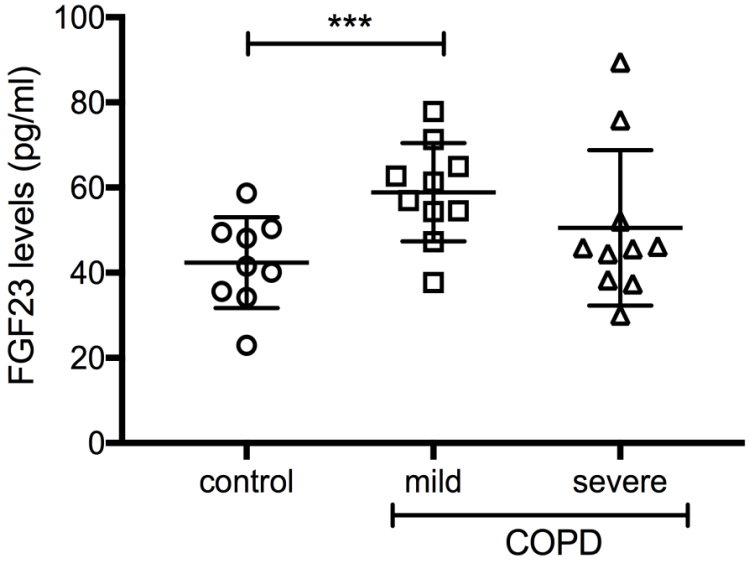
***
FGF23 levels (pg/ml)
100
80
60
40
20
0
control
mild
severe
COPD

b

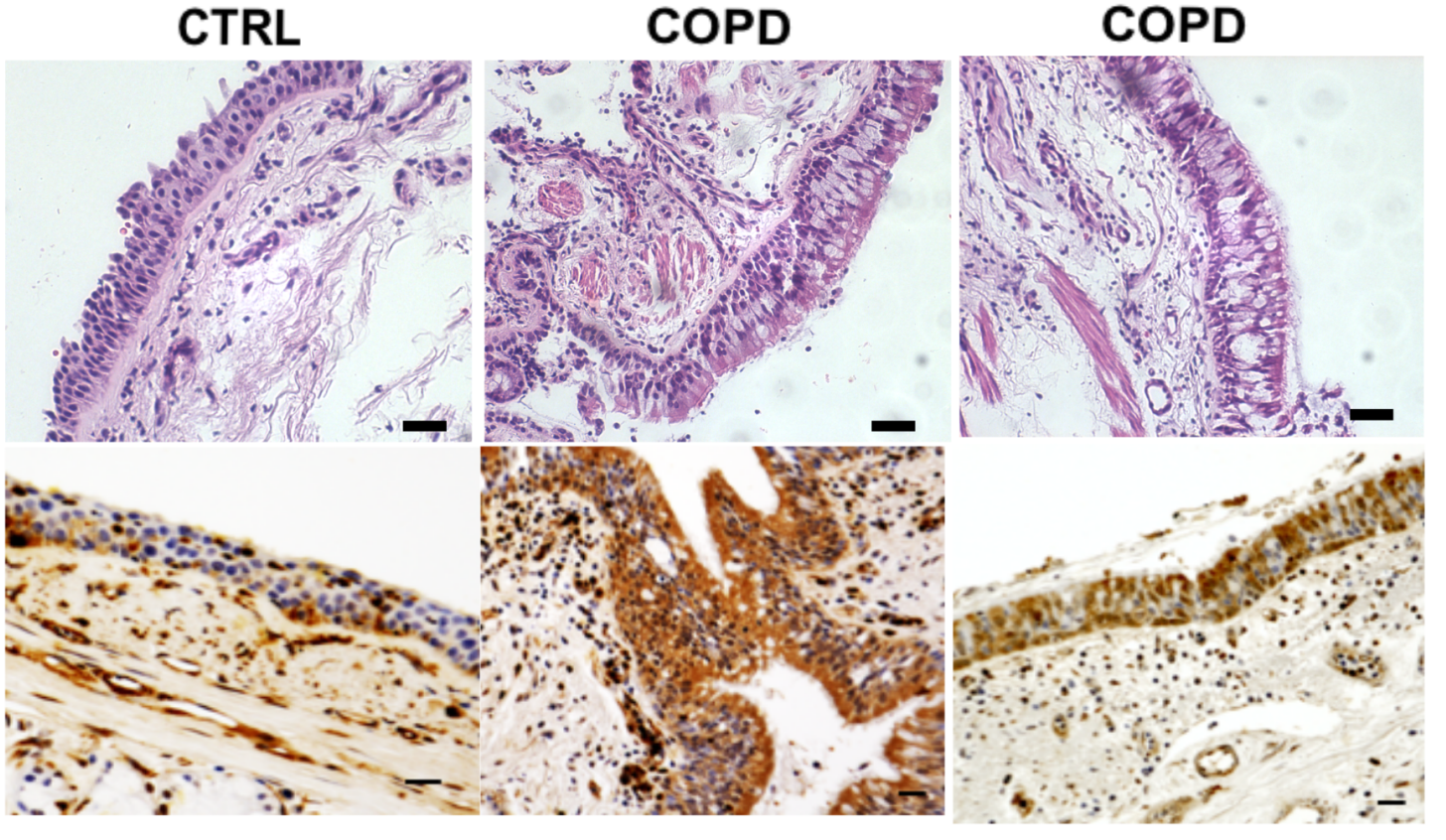
CTRL
COPD
COPD

c

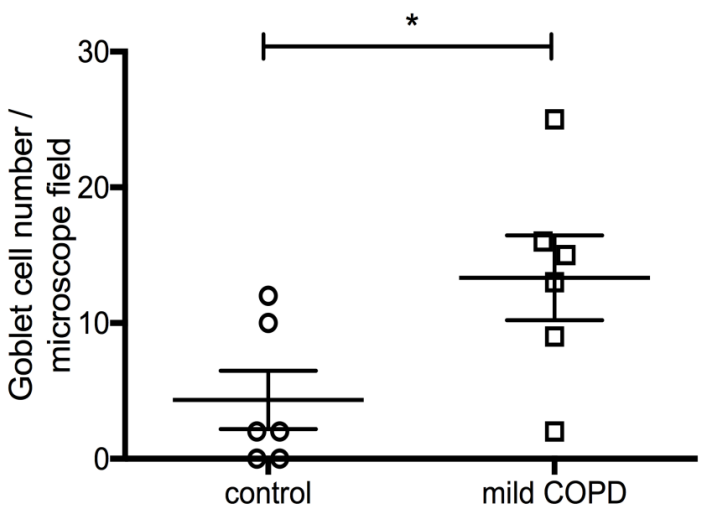
*
Goblet cell number / microscope field
30
20
10
0
control
mild COPD

d

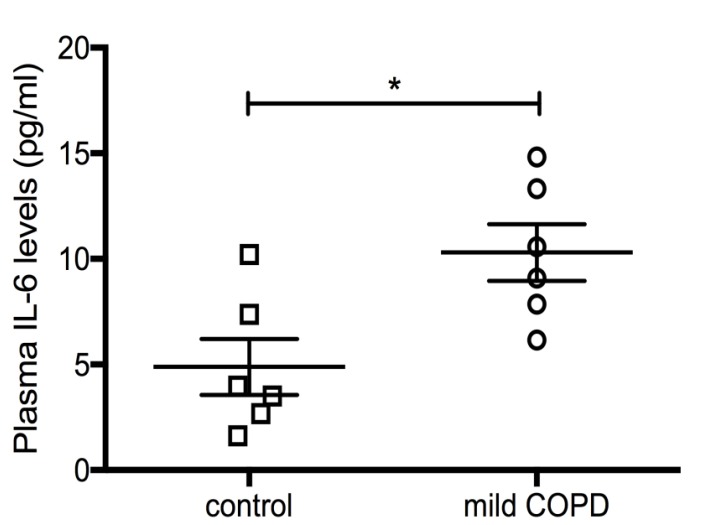
*
Plasma IL-6 levels (pg/ml)
20
15
10
5
0
control
mild COPD

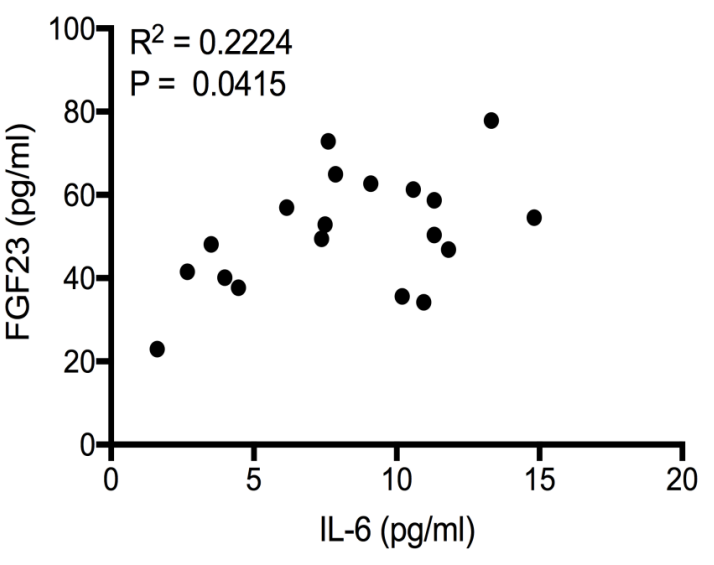
R2 = 0.2224
P = 0.0415
FGF23 (pg/ml)
100
80
60
40
20
0
0
5
10
15
20
IL-6 (pg/ml)

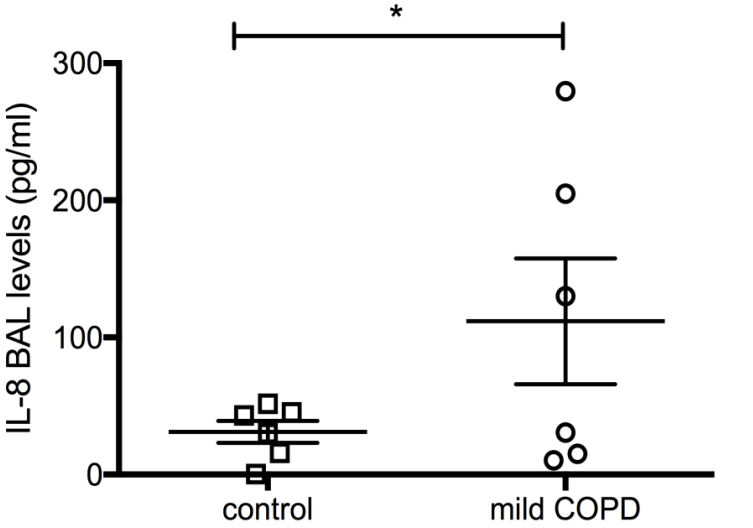
*
IL-8 BAL levels (pg/ml)
300
200
100
0
control
mild COPD

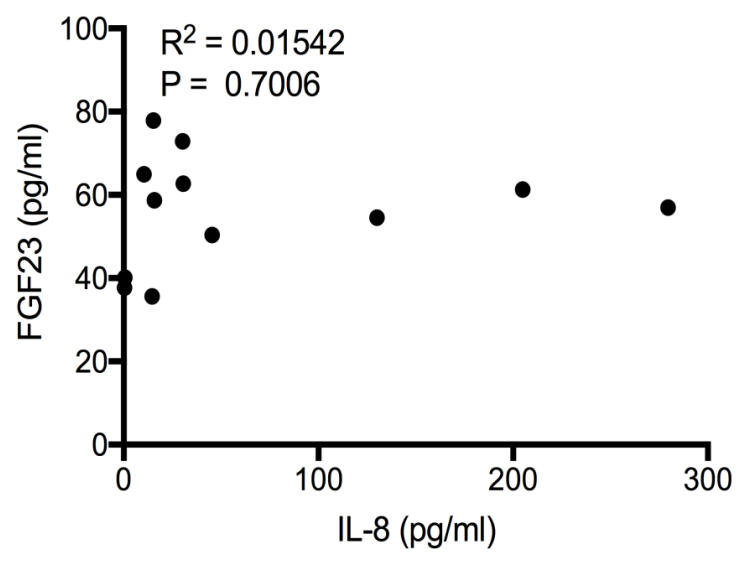
R2 = 0.01542
P = 0.7006
FGF23 (pg/ml)
100
80
60
40
20
0
0
100
200
300
IL-8 (pg/ml)

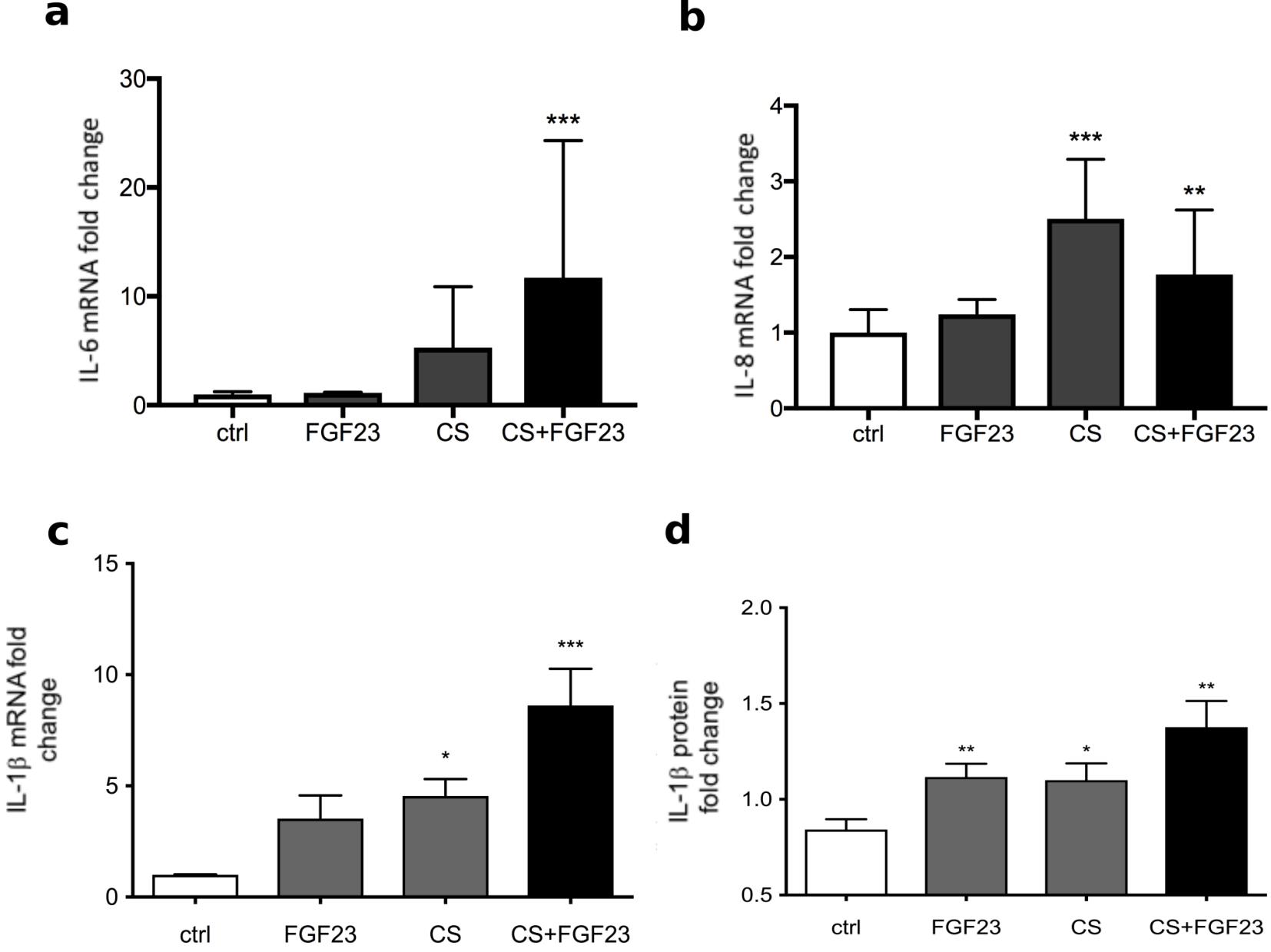
a
IL-6 mRNA fold change
30
20
10
0
***
ctrl
FGF23
CS
CS+FGF23
b
IL-8 mRNA fold change
4
3
2
1
0
***
**
ctrl
FGF23
CS
CS+FGF23
c
IL-1β mRNA fold change
15
10
5
0
*
***
ctrl
FGF23
CS
CS+FGF23
d
IL-1β protein fold change
2.0
1.5
1.0
0.5
**
*
**
ctrl
FGF23
CS
CS+FGF23

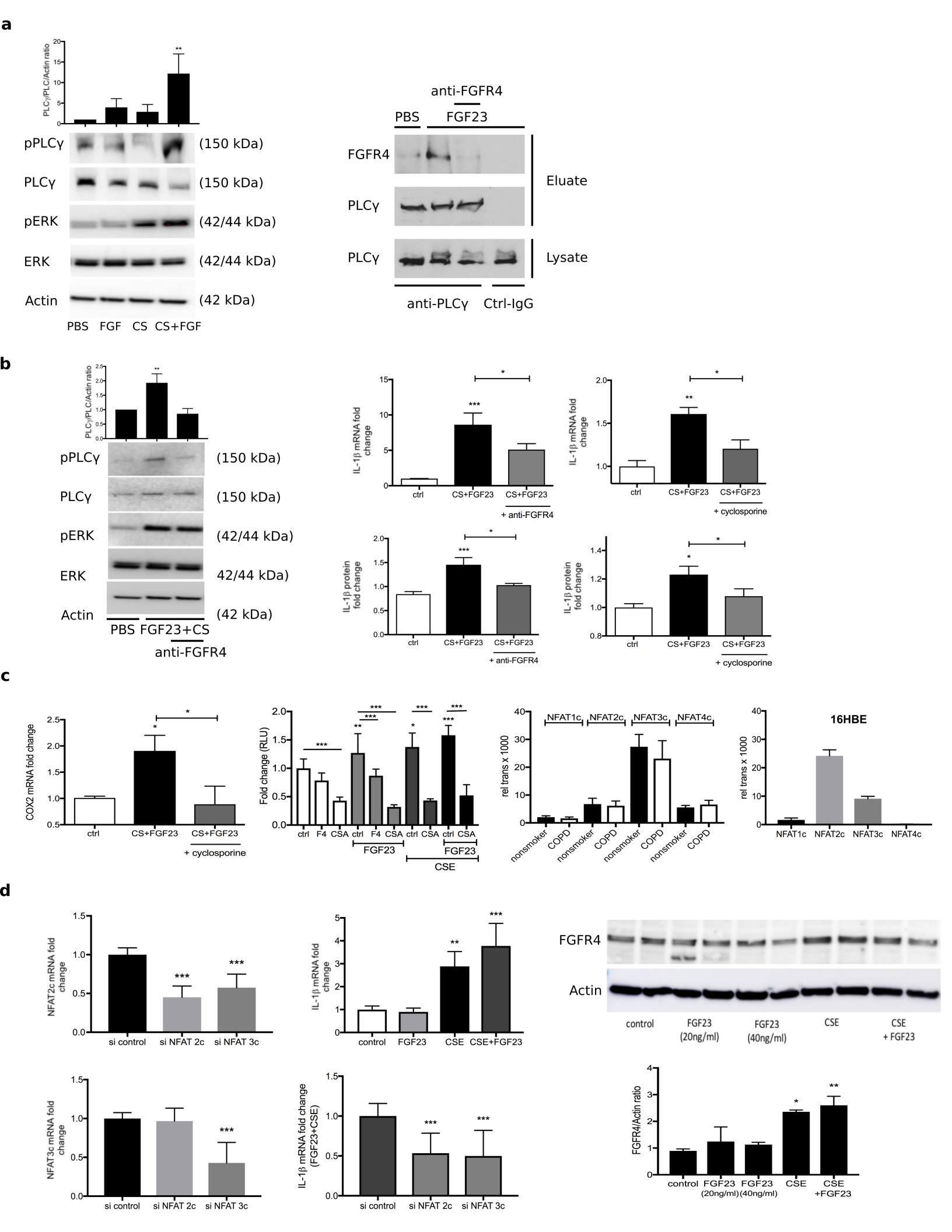
a
PLCγ/PLC/Actin ratio
pPLCγ (150 kDa)
PLCγ (150 kDa)
pERK (42/44 kDa)
ERK (42/44 kDa)
Actin (42 kDa)
PBS FGF CS CS+FGF
anti-FGFR4
PBS FGF23
FGFR4
PLCγ
Eluate
PLCγ
Lysate
anti-PLCγ Ctrl-IgG
b
PLCγ/PLC/Actin ratio
pPLCγ (150 kDa)
PLCγ (150 kDa)
pERK (42/44 kDa)
ERK 42/44 kDa)
Actin (42 kDa)
PBS FGF23+CS
anti-FGFR4
IL-1β mRNA fold change
ctrl CS+FGF23 CS+FGF23
+ anti-FGFR4
IL-1β mRNA fold change
ctrl CS+FGF23 CS+FGF23
+ cyclosporine
IL-1β protein fold change
ctrl CS+FGF23 CS+FGF23
+ anti-FGFR4
IL-1β protein fold change
ctrl CS+FGF23 CS+FGF23
+ cyclosporine
c
COX2 mRNA fold change
ctrl CS+FGF23 CS+FGF23
+ cyclosporine
Fold change (RLU)
ctrl F4 CSA ctrl F4 CSA ctrl CSA ctrl CSA
FGF23
FGF23
CSE
rel trans x 1000
NFAT1c NFAT2c NFAT3c NFAT4c
nonsmoker COPD nonsmoker COPD nonsmoker COPD nonsmoker COPD
16HBE
rel trans x 1000
NFAT1c NFAT2c NFAT3c NFAT4c
d
NFAT2c mRNA fold change
si control si NFAT 2c si NFAT 3c
IL-1β mRNA fold change
control FGF23 CSE CSE+FGF23
FGFR4
Actin
control FGF23 (20ng/ml) FGF23 (40ng/ml) CSE CSE + FGF23
NFAT3c mRNA fold change
si control si NFAT 2c si NFAT 3c
IL-1β mRNA fold change (FGF23+CSE)
si control si NFAT 2c si NFAT 3c
FGFR4/Actin ratio
control FGF23 (20ng/ml) FGF23 (40ng/ml) CSE CSE +FGF23

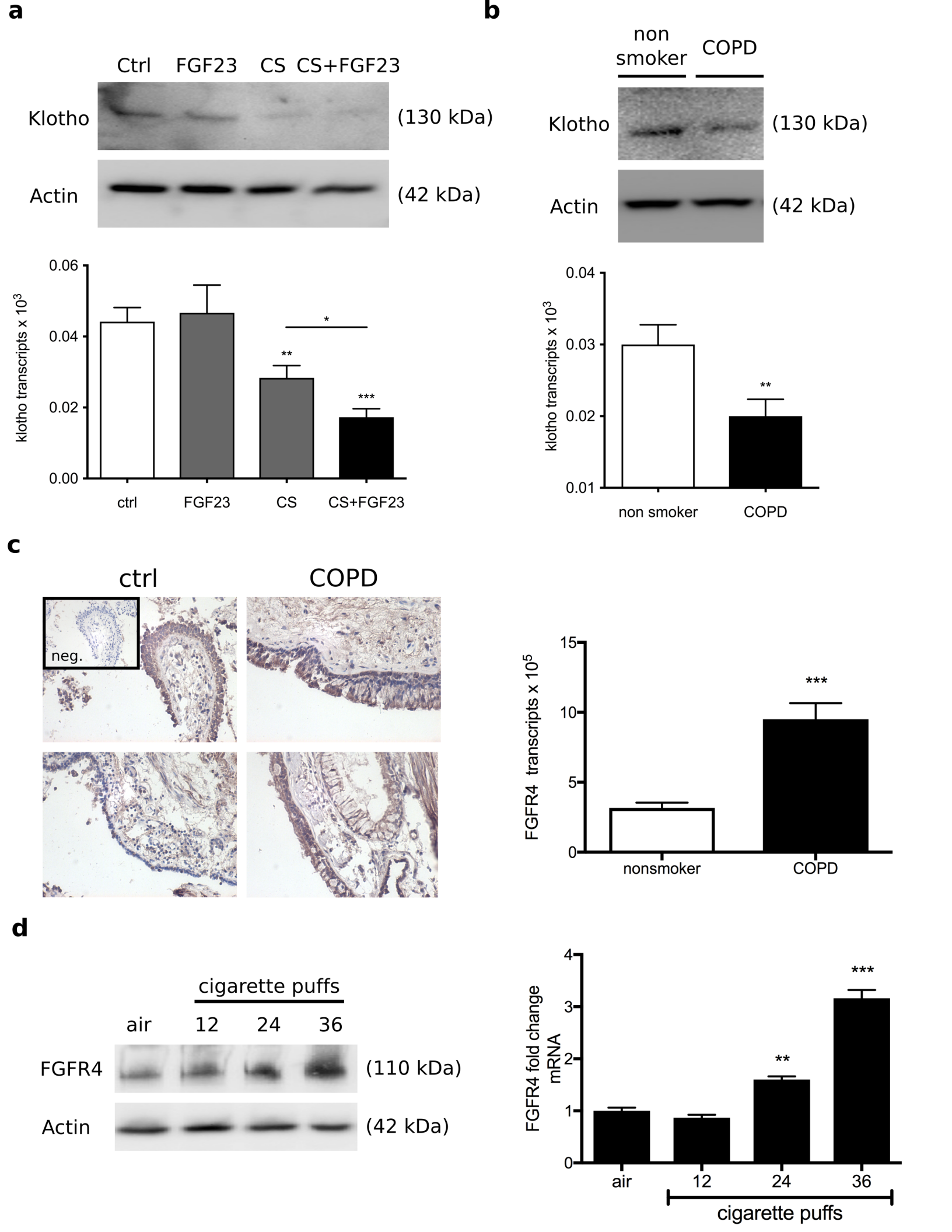
a
Ctrl
FGF23
CS
CS+FGF23
Klotho
(130 kDa)
Actin
(42 kDa)
klotho transcripts x 10^3
0.06
0.04
0.02
0.00
*
**
***
ctrl
FGF23
CS
CS+FGF23
b
non smoker
COPD
Klotho
(130 kDa)
Actin
(42 kDa)
klotho transcripts x 10^3
0.04
0.03
0.02
0.01
**
non smoker
COPD
c
ctrl
COPD
neg.
FGFR4 transcripts x 10^5
15
10
5
0
***
nonsmoker
COPD
d
cigarette puffs
air
12
24
36
FGFR4
(110 kDa)
Actin
(42 kDa)
FGFR4 fold change mRNA
4
3
2
1
0
**
***
air
12
24
36
cigarette puffs

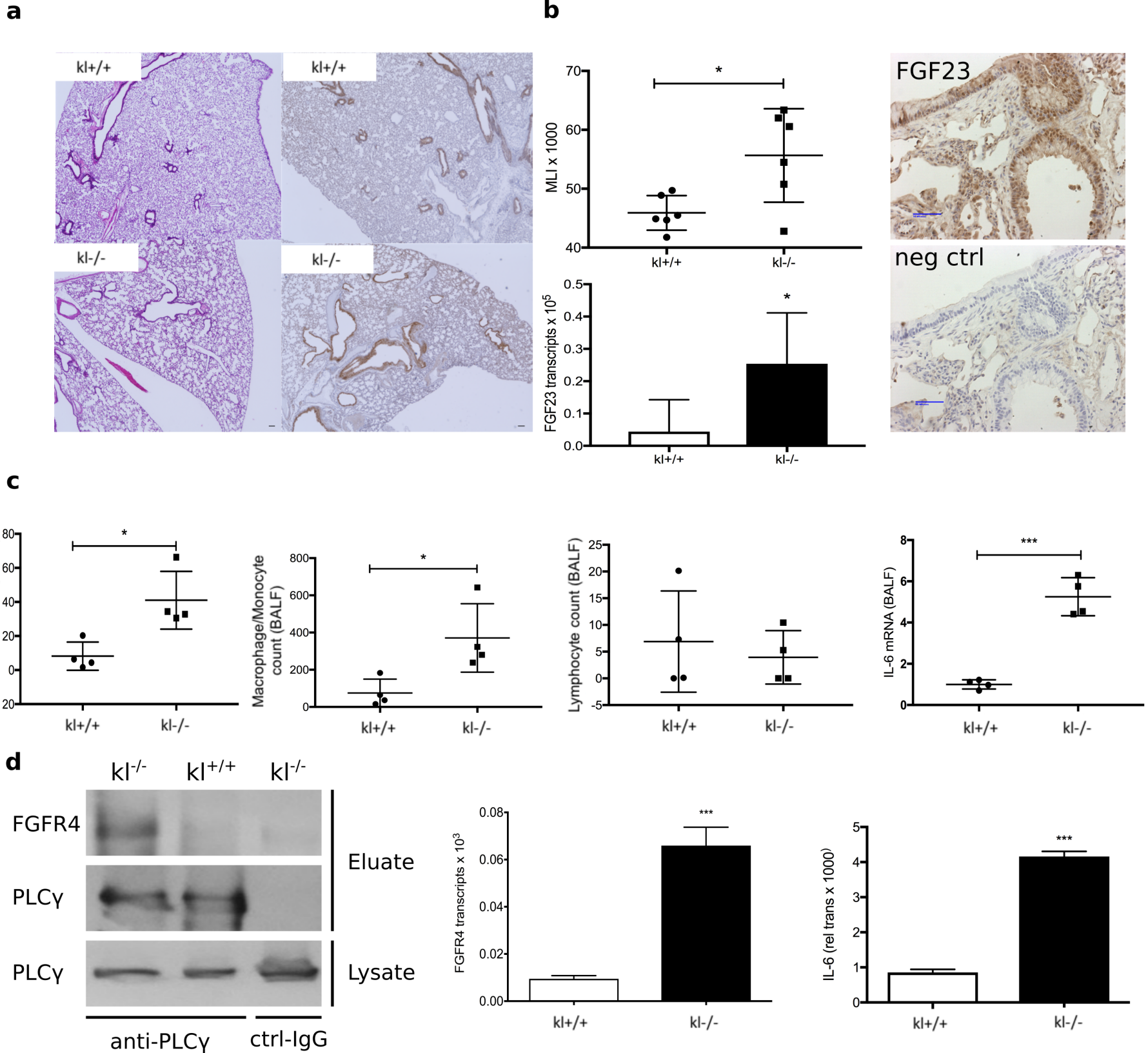
a
kl+/+
kl+/+
kl-/-
kl-/-
b
MLI x 1000
70
60
50
40
*
kl+/+
kl-/-
FGF23 transcripts x 10^5
0.5
0.4
0.3
0.2
0.1
0.0
*
kl+/+
kl-/-
FGF23
neg ctrl
c
Total cell count (BALF)
80
60
40
20
0
20
*
kl+/+
kl-/-
Macrophage/Monocyte count (BALF)
800
600
400
200
0
*
kl+/+
kl-/-
Lymphocyte count (BALF)
25
20
15
10
5
0
-5
kl+/+
kl-/-
IL-6 mRNA (BALF)
8
6
4
2
0
***
kl+/+
kl-/-
d
kl-/-
kl+/+
kl-/-
FGFR4
PLCγ
PLCγ
Eluate
Lysate
anti-PLCγ
ctrl-IgG
FGFR4 transcripts x 10^3
0.08
0.06
0.04
0.02
0.00
***
kl+/+
kl-/-
IL-6 (rel trans x 1000)
5
4
3
2
1
0
***
kl+/+
kl-/-

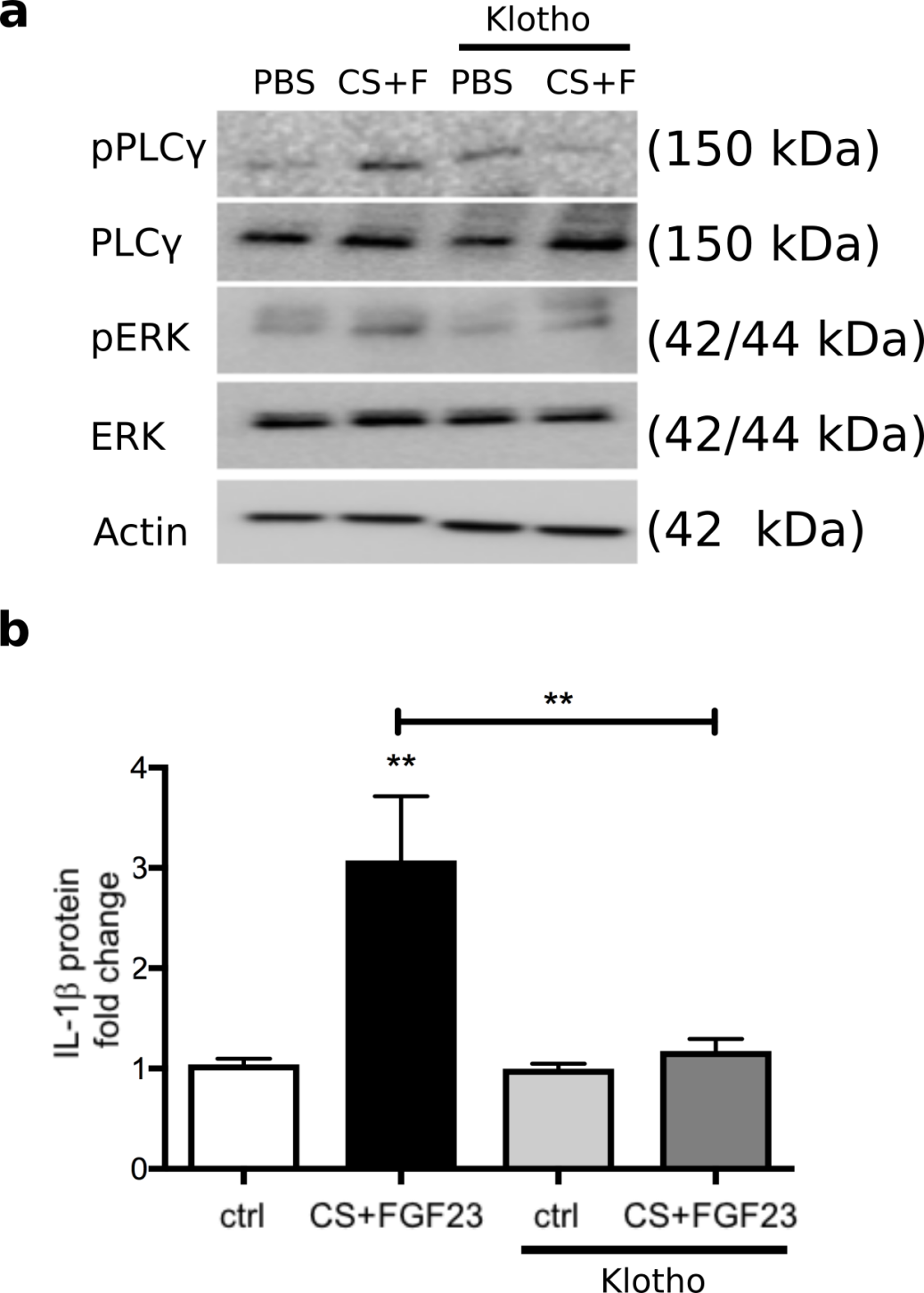
a
Klotho
PBS
CS+F
PBS
CS+F
pPLCγ
(150 kDa)
PLCγ
(150 kDa)
pERK
(42/44 kDa)
ERK
(42/44 kDa)
Actin
(42 kDa)
b
**
**
IL-1β protein fold change
4
3
2
1
0
ctrl
CS+FGF23
ctrl
CS+FGF23
Klotho

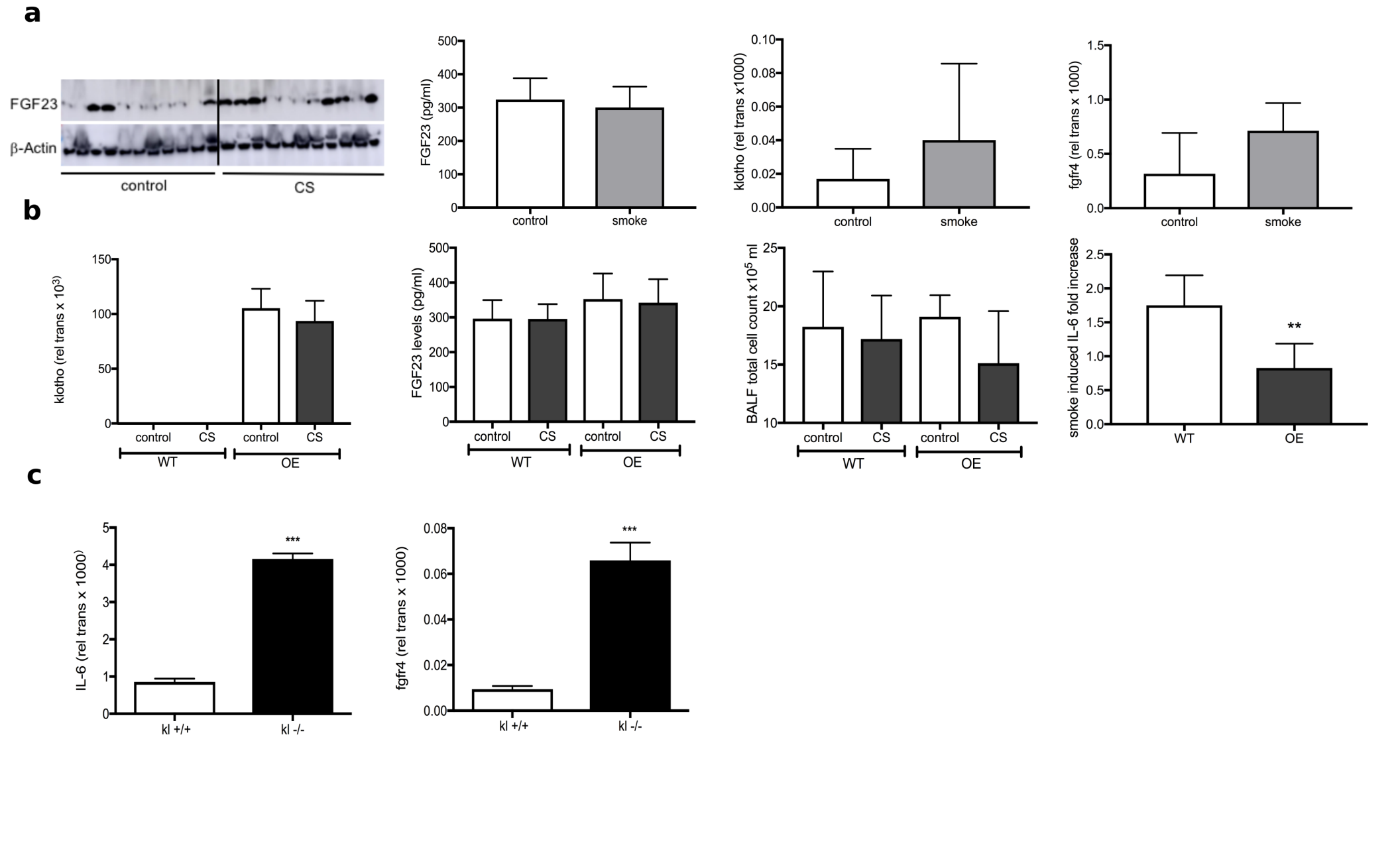
a
FGF23
β-Actin
control
CS
FGF23 (pg/ml)
control
smoke
klotho (rel trans x1000)
fgfr4 (rel trans x 1000)
b
klotho (rel trans x 10³)
WT
OE
FGF23 levels (pg/ml)
BALF total cell count x10⁵ ml
smoke induced IL-6 fold increase
**
c
IL-6 (rel trans x 1000)
***
kl +/+
kl -/-
fgfr4 (rel trans x 1000)

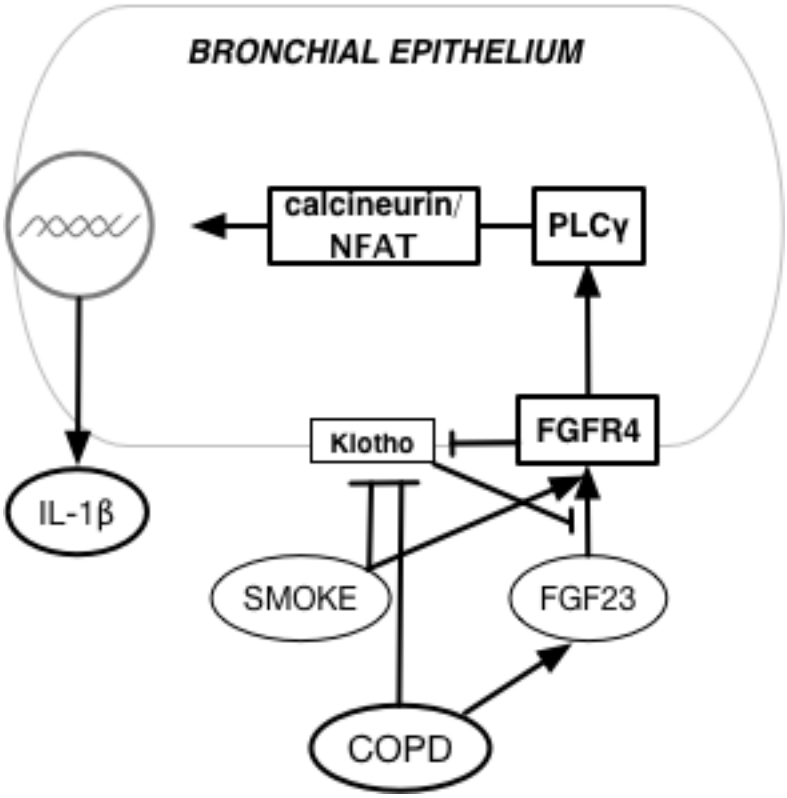
BRONCHIAL EPITHELIUM
calcineurin/
NFAT
PLCγ
FGFR4
Klotho
IL-1β
SMOKE
FGF23
COPD

ONLINE DATA SUPPLEMENT

Study Design

Subjects were recruited from pulmonary clinics and by advertising locally. Inclusion criteria included males and females, > 40 years, either nonsmokers or smokers of at least 10 pack-years in their lifetime. All subjects considered former smokers had to be abstinent of tobacco use for at least 12 months; whereas active smokers had to smoke at least one cigarette within 3 days of enrollment. Participation exclusion criteria included self-reported evidence of heart disease, creatinine elevation above normal reference value, use of antibiotics, systemic steroids or immunosuppressant agents within 12 weeks, presence of an exacerbation or acute upper respiratory infection within the previous 4 weeks and history of any lung condition other than COPD such as bronchiectasis, asthma, pulmonary malignancies or prior thoracic surgery. In addition, subjects had to be in stable clinical condition to undergo a bronchoscopy as per the physician investigators. All subjects underwent complete pulmonary function testing and filled in a detailed clinical and demographic questionnaire. We classified all smokers with airflow obstruction ($FEV_1/FVC \leq 0.70$) as having COPD.

Antibodies

anti-rabbit α-klotho Ab, Abcam (Cambridge, MA, USA)

anti-rabbit FGFR4 antibody (sc-124), Santa Cruz Biotechnology, Dallas, TX, USA

anti-goat α-klotho antibody (sc-22220), Santa Cruz Biotechnology, Dallas, TX, USA

anti-rabbit phospho-PLCγ (8713S), Cell Signaling, Danvers, MA, USA

anti-rabbit PLCγ (2822S), Cell Signaling, Danvers, MA, USA

anti-β-actin antibody, Sigma-Aldrich, St. Louis, MO, USA

anti-rabbit phospho-ERK (9101S), Cell Signaling, Danvers, MA, USA

anti-rabbit ERK (4695S), Cell Signaling, Danvers, MA, USA

Bronchoalveolar lavage and venipuncture

All subjects underwent bronchoscopy via the nasal passage using a single flexible bronchoscope (Olympus, PA, USA) under conscious sedation in accordance with standard clinical practice. After the vocal cords and trachea were anesthetized with 1% lidocaine, the bronchoscope was directly inserted into the right middle lobe bronchus and wedged. Bronchoalveolar lavage (BAL) was collected with three instillations of 20 cc of saline and immediately aspirated using a collector trap on the suction port of the scope, centrifuged and the supernatant stored in 1 ml aliquots at -80^{o}C until analyzed. Transbronchial biopsies were obtained as well. The patients also underwent venipuncture and 5 ml of blood was collected, centrifuged at 1500 rpm for 5 minutes and the serum was stored in aliquots at -80^{o}C until analyzed.

RNA Extraction and Quantitative RT-PCR

Total RNA was extracted from ALI-cultured human airway epithelial cells using the RNeasy Protect mini kit (Qiagen, Valencia, CA, USA). Reverse transcription was done using the iScript cDNA synthesis kit (Bio-Rad, Hercules, CA, USA) with 1 μg of RNA according to the instructions of the manufacturer. Real-time quantitative PCR was performed using the following TaqMan probes: Hs00174097_m1 for IL-1β,

Hs00873651_m1 for MUC5AC, Hs00174103_m1 for IL-8, and Hs02758991_g1 for GAPDH.

Western Blotting

ALI-cultured human airway epithelial cells were lysed in radioimmune precipitation assay buffer containing protease inhibitors. Protein yield was measured by BCA assay (Pierce). Proteins were separated on a 4–20% precast Ready Gel (Bio-Rad) and blotted onto Immobilon-P membranes (Millipore, Billerica, MA). Membranes were blocked with 5% nonfat dry milk in Tris-buffered saline (pH 7.4) with 0.05% Tween 20 (TTBS) for 1 h. Primary antibodies were as follows: rabbit anti- phospho PLCγ and PLCγ antibodies (Cell Signaling), used as prescribed previously (1,2); rabbit total and phosphor-ERK1/2 (Cell Signaling); rabbit anti-FGFR4 and mouse anti-β-actin antibody. Secondary antibody was an anti-rabbit (Seracare, Milford, MA, USA) or anti-mouse (Seracare, Milford, MA, USA) horseradish peroxidase-linked antibody used at 1:5000 in TTBS for 1 h at room temperature. Positive signals were visualized by chemiluminescence on a ChemiDoc XRS system (Bio-Rad, Hercules, CA, USA).

16 HBE Cell Culture

16HBE cells, a SV40-immortalized human bronchial epithelial cell line, generously provided by the UAB Cystic Fibrosis Center, were utilized for this study. Cells were grown in Eagle's Minimum Essential Medium (EMEM) supplemented with 10% heat-inactivated fetal bovine serum (Atlas Biologicals; Fort Collins, CO) and without antibiotics, hereafter referred to as complete medium (CM).

NFAT Luciferase Reporter Assay

To access NFAT transcriptional activity following FGF23 treatment, 16HBE cells were seeded at a density of 1.5 x10^4cells/well in 96-well plates. After 24 hours, cells were transfected with the constitutively-active *Renilla*-luciferase construct, as a transfection control, along with 100 ng/well of a Fire Fly Luciferase reporter construct, either a NFAT reporter or a null promoter construct serving as a negative control as provided with the NFAT Cignal Reporter Assay Kit (Qiagen; Hilden, Germany). Transfection was performed under serum-free conditions in OptiMEM using Lipofectamine 2000 transfection reagent (Thermo Scientific, Grand Island, NY, USA). After an overnight incubation, the medium was replaced with CM. When required, cells were pre-incubated for 30 min with 10 μM of the FGFR4 inhibitor BLU9931 (Selleck Chemicals, Houston, TX, USA). Immediately thereafter, varying dilutions of recombinant human FGF23 in the presence or absence of BLU9931 were added to the wells. Following an additional 24 hr incubation, a Luciferase assay was performed using the Dual-Luciferase Reporter Assay System (Promega; Madison, WI, USA) as directed by the manufacturer. Briefly, the cells were washed with phosphate buffered saline, pH 7.4 (PBS), then lysed in 80 μL of passive lysis buffer at room temperature with shaking for 15 min. 20 μL lysate was loaded into each well of an opaque 96-well plate and relative light units were measured utilizing a SpectraMax i3x plate reader equipped with dual injectors (Molecular Devices; Sunnyvale, CA, USA).

NFAT knockdown Experiments

The effect of NFAT knockdown on IL-1β induction following FGF23 and cigarette smoke extract (CSE) treatment was tested on 16HBE cells. 6 x 10^4 cells were seeded in 24-well plates. The next day, medium was replaced with 0.5mL OptiMEM (Thermo Scientific, Grand Island, NY, USA) and the cells were transfected with 5 nmol of either AllStar negative control, a mix of two NFATC2 siRNAs, or a mix of two NFATC3 siRNAs using 3 μL/well of HiPerFect transfection reagent (Qiagen; Hilden, Germany). Following a 6 hour incubation, medium was replaced following an additional 48 hr incubation to allow for NFAT knockdown, cells were treated with FGF-23 (40 ng/mL), 5% CSE or vehicle (DMSO or CM) control. After 24 hours, wells were washed with 1.0 mL cold phosphate buffered saline (pH 7.4) and RNA was extracted using the GeneJET RNA purification kit (Thermo Scientific, Grand Island, NY, USA). cDNA was generated using the Maxima H Minus First Strand cDNA Synthesis Kit and transcript levels for NFAT and IL-1β were quantified using Taqman assays (Thermo Scientific, Grand Island, NY, USA).

Morphometric Analysis and BALF in mice

Morphometric analyses were conducted in a standard fashion as previously reported assessing mean linear intercepts after fixation of the murine lung tissue (3). BALF was obtained following established protocols of the lab (4). Briefly, a tracheal cannula was inserted and the BAL procedure was performed under direct visualization of lung distension (maximum 2 ml), as previously described (5,6). Cells were pelleted by centrifugation (1,100 × *g* for 5 min at 4° C), resuspended in PBS and stained with modified Wright-Giemsa for differential cell counts.

Air-liquid interface (ALI) cell culture and cigarette smoke exposure

Human bronchial epithelial cells (HBEC) from age-matched nonsmoker and COPD lungs were isolated and de-differentiated through expansion as described previously (7,8). Fully differentiated HBEC were exposed to cigarette smoke (Kentucky 3R4F cigarettes) using a Vitrocell VC-10 smoking robot (Vitrocell Systems GMBH, Waldkirch, Germany) (8). Murine tracheal epithelial cells (MTEC) were obtained from wild type mice as well as klotho hypomorphic mice (SV129 background) (9). MTEC from wild type and kl+/-, kl-/- mice (10)were cultured and differentiated according to an adapted protocol of You et al. (7,11). Cells were fully differentiated after approximately 2-3 weeks and then used for experiments.

Acute cigarette smoke exposure in mice

Klotho overexpressing mice and their wild type littermates (10) were exposed to cigarette smoke (3R4F, University of Kentucky) twice daily (1 hour smoke – 1h break – 1h smoke) for a total of 5 days with increasing amounts of cigarettes (Day 1: 4 cigarettes/day, Day 2: 6 cigarettes/day, Day3: 8 cigarettes/day, Day 4: 10 cigarettes/day and Day 5: 12 cigarettes/day).

1. Grabner, A., Amaral, A. P., Schramm, K., Singh, S., Sloan, A., Yanucil, C., Li, J., Shehadeh, L. A., Hare, J. M., David, V., Martin, A., Fornoni, A., Di Marco, G. S., Kentrup, D., Reuter, S., Mayer, A. B., Pavenstadt, H., Stypmann, J., Kuhn, C., Hille, S., Frey, N., Leifheit-Nestler, M., Richter, B., Haffner, D., Abraham, R., Bange, J., Sperl, B., Ullrich, A., Brand, M., Wolf, M., and Faul, C. (2015) Activation of Cardiac Fibroblast Growth Factor Receptor 4 Causes Left Ventricular Hypertrophy. *Cell metabolism* **22**, 1020-1032
2. Krick, S., Wang, J., St-Pierre, M., Gonzalez, C., Dahl, G., and Salathe, M. (2016) Dual Oxidase 2 (Duox2) Regulates Pannexin 1-mediated ATP Release in

Primary Human Airway Epithelial Cells via Changes in Intracellular pH and Not H2O2 Production. *The Journal of biological chemistry* **291**, 6423-6432
3. Shiomi, T., Okada, Y., Foronjy, R., Schiltz, J., Jaenish, R., Krane, S., and D'Armiento, J. (2003) Emphysematous changes are caused by degradation of type III collagen in transgenic mice expressing MMP-1. *Exp Lung Res* **29**, 1-15
4. Foronjy, R. F., Salathe, M. A., Dabo, A. J., Baumlin, N., Cummins, N., Eden, E., and Geraghty, P. (2016) TLR9 expression is required for the development of cigarette smoke-induced emphysema in mice. *American journal of physiology. Lung cellular and molecular physiology* **311**, L154-166
5. Weathington, N. M., van Houwelingen, A. H., Noerager, B. D., Jackson, P. L., Kraneveld, A. D., Galin, F. S., Folkerts, G., Nijkamp, F. P., and Blalock, J. E. (2006) A novel peptide CXCR ligand derived from extracellular matrix degradation during airway inflammation. *Nat Med* **12**, 317-323
6. Wells, J. M., O'Reilly, P. J., Szul, T., Sullivan, D. I., Handley, G., Garrett, C., McNicholas, C. M., Roda, M. A., Miller, B. E., Tal-Singer, R., Gaggar, A., Rennard, S. I., Jackson, P. L., and Blalock, J. E. (2014) An aberrant leukotriene A4 hydrolase-proline-glycine-proline pathway in the pathogenesis of chronic obstructive pulmonary disease. *Am J Respir Crit Care Med* **190**, 51-61
7. Chen, X., Baumlin, N., Buck, J., Levin, L. R., Fregien, N., and Salathe, M. (2014) A soluble adenylyl cyclase form targets to axonemes and rescues beat regulation in soluble adenylyl cyclase knockout mice. *American journal of respiratory cell and molecular biology* **51**, 750-760
8. Schmid, A., Baumlin, N., Ivonnet, P., Dennis, J. S., Campos, M., Krick, S., and Salathe, M. (2015) Roflumilast partially reverses smoke-induced mucociliary dysfunction. *Respiratory research* **16**, 135
9. Kuro-o, M., Matsumura, Y., Aizawa, H., Kawaguchi, H., Suga, T., Utsugi, T., Ohyama, Y., Kurabayashi, M., Kaname, T., Kume, E., Iwasaki, H., Iida, A., Shiraki-Iida, T., Nishikawa, S., Nagai, R., and Nabeshima, Y. I. (1997) Mutation of the mouse klotho gene leads to a syndrome resembling ageing. *Nature* **390**, 45-51
10. Li, Q., Vo, H. T., Wang, J., Fox-Quick, S., Dobrunz, L. E., and King, G. D. (2017) Klotho regulates CA1 hippocampal synaptic plasticity. *Neuroscience* **347**, 123-133
11. You, Y., and Brody, S. L. (2013) Culture and differentiation of mouse tracheal epithelial cells. *Methods in molecular biology* **945**, 123-143

SUPPLEMENTARY FIGURE LEGENDS

Table 1

Patient characteristics of our study population, divided into patients without (FEV1/FVC > 0.7) and with mild – moderate or severe COPD (FEV1/FVC < 0.7), including age, gender, FEV1 % predicted post bronchodilator, smoking status and FGF23 plasma levels (shown as mean ± S.E.M.).

Supplementary Figure 1. (a) Dot plot showing plasma FGF23 levels in the control cohort, subdivided in 5 non-smokers and 5 active smokers showing no significant difference when unpaired Student's t-test was used for comparison ($p = 0.1047$). (b) Bar graphs indicating serum FGF23 levels in control mice compared to mice exposed to cigarette smoke for a total of 6 months (3 mice per group). (shown as mean ± S.E.M. with ***$p<0.005$).

Supplementary Figure 2. (a) mRNA levels of IL-6 and (b) klotho in fgfr4 WT and TG MTECs. (c) IL6 and klotho mRNA fold change 24h after stimulation with cigarette smoke (2 cigarettes) ± FGF23 (25 ng/ml) in MTECs from $fgfr4^{+/+}$ and $fgfr4^{-/-}$ MTECs. (d) fgfr4 transcript levels in $fgfr4^{+/+}$ and $fgfr4^{-/-}$ MTECs. All bar graphs are mean ± S.E.M. *$P<0.05$, **$P<0.01$ and ***$P<0.005$, compared to control (ctrl) group.

Supplemental Table 1. Clinical Characteristics

	Non-COPD (n = 10)	Mild-to-moderate COPD (n = 9)	Severe COPD (n = 9)	P value
Age, years	53 ± 9	57 ± 10	63 ± 2	(p=0.29, p=0.02)
Male sex	3 (33%)	8 (80%)	8 (80%)	(p=0.008, p<0.008)
FEV1%	100 ± 17	64 ± 15	44 ± 17	(p=0.0002, p<0.0001)
Current smoker	5 (56%)	4 (40%)	2 (20%)	(p>0.9999, p=0.45)
FGF23 (pg/ml)	42 ± 10	59 ± 12	51 ± 18	(p=0.004, p=0.42)

Data expressed as mean ± standard deviation or n (%). FEV1% = post-bronchodilator forced-expiratory volume in 1-second percent predicted. P values show comparison of control vs mild-moderate COPD and control vs severe COPD using 1-way ANOVA and either Tukey post test or Kruskal Wallis (for gender and smoking status).

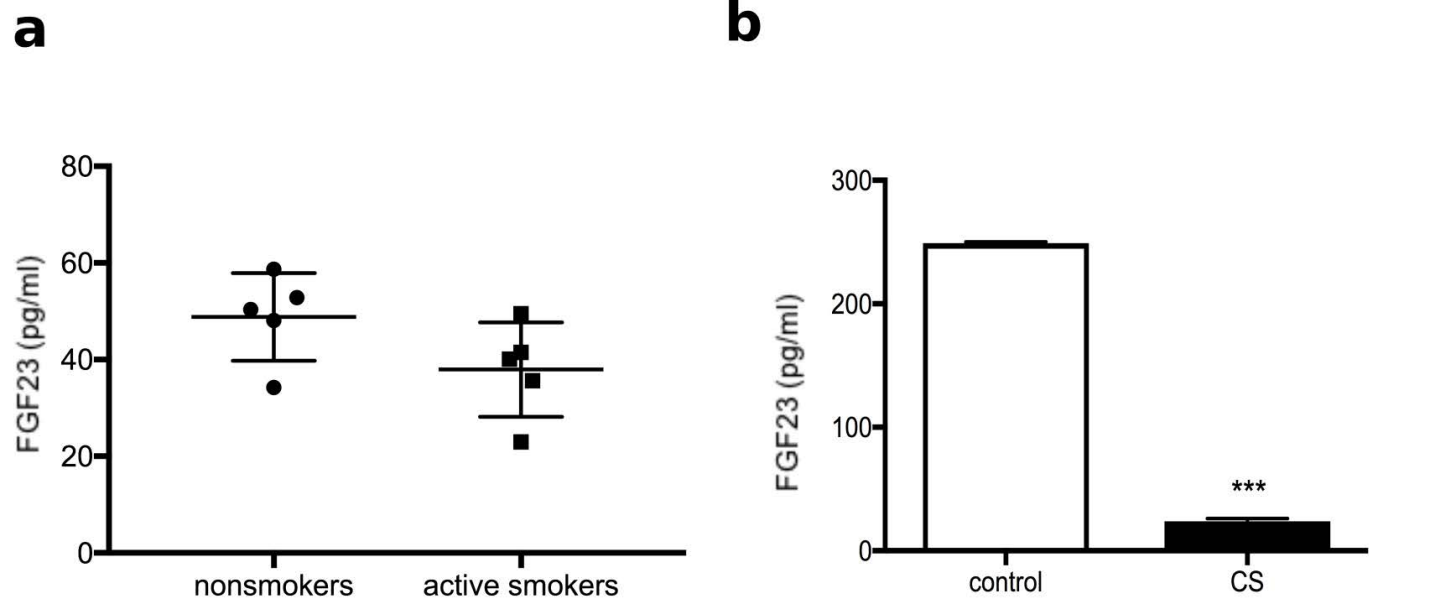
a
80
60
40
20
0
FGF23 (pg/ml)
nonsmokers
active smokers
b
300
200
100
0
FGF23 (pg/ml)
***
control
CS

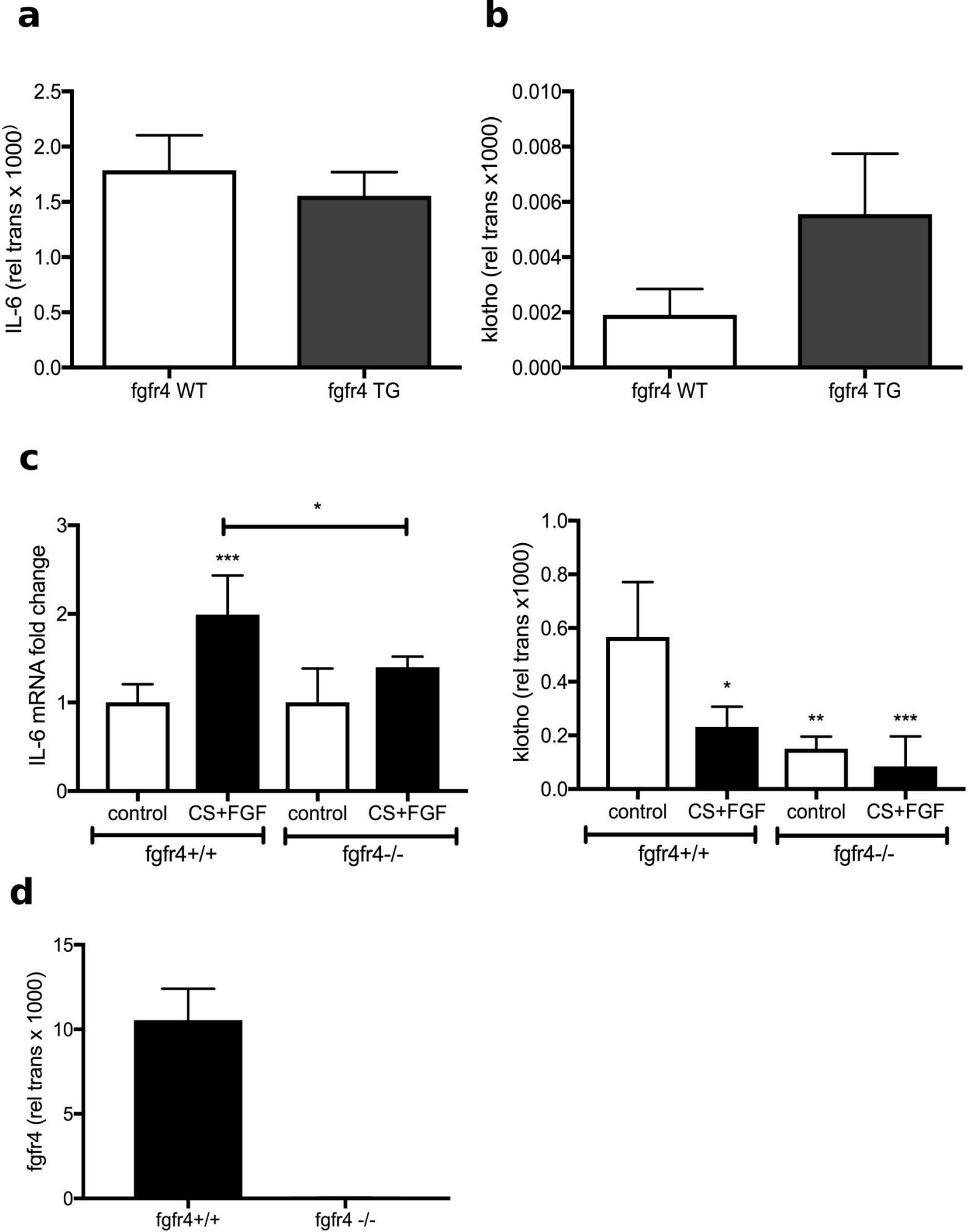
a
IL-6 (rel trans x 1000)
2.5
2.0
1.5
1.0
0.5
0.0
fgfr4 WT
fgfr4 TG
b
klotho (rel trans x1000)
0.010
0.008
0.006
0.004
0.002
0.000
fgfr4 WT
fgfr4 TG
c
IL-6 mRNA fold change
3
2
1
0
*
***
control
CS+FGF
control
CS+FGF
fgfr4+/+
fgfr4-/-
klotho (rel trans x1000)
1.0
0.8
0.6
0.4
0.2
0.0
*
**
***
control
CS+FGF
control
CS+FGF
fgfr4+/+
fgfr4-/-
d
fgfr4 (rel trans x 1000)
15
10
5
0
fgfr4+/+
fgfr4 -/-